AMERICAN UNIVERSITY OF BEIRUT

AC NETWORK PLANNING OF MICROGRIDS WITH STORAGE AND RENEWABLE ENERGY

by
MOHAMMAD KHALIL YOUSSEF FATTOUH

A thesis
submitted in partial fulfillment of the requirements
for the degree of Master of Engineering
to the Department of Electrical and Computer Engineering
of the Maroun Semaan Faculty of Engineering and Architecture
at the American University of Beirut

Beirut, Lebanon
August 2024

AMERICAN UNIVERSITY OF BEIRUT

AC NETWORK PLANNING OF MICROGRIDS WITH STORAGE AND RENEWABLE ENERGY

by

MOHAMMAD KHALIL YOUSSEF FATTOUH

Approved by:

Dr. Sami Karaki, Professor Department of Electrical and Computer Engineering	Advisor
Dr. Rabih Jabr, Professor Department of Electrical and Computer Engineering	Member of Committee
Dr. Dany Abou Jaoude, Assistant Professor Department of Mechanical Engineering	Member of Committee

Date of thesis defense: August 28, 2024

ACKNOWLEDGEMENTS

I would like to express my deepest gratitude to my thesis advisor, Prof. Sami Karaki, for his invaluable guidance, insightful feedback, and unwavering support throughout my thesis paper. His expertise and encouragement have been instrumental in shaping the direction and quality of this work.

I am also profoundly thankful to my father, mother, and sister for their love, patience, and encouragement. Their belief in me has been a constant source of motivation, and their support has served as the foundation upon which I have built this journey. Additionally, I would like to acknowledge every person who motivated me to pursue my passion and continue my studies. Your words and actions have inspired me to strive for excellence, and for that I am truly grateful.

ABSTRACT
OF THE THESIS OF

Mohammad Khalil Youssef Fattouh for Master of Engineering
Major: Power and Energy System

Title: AC Network Planning of Microgrids with Storage and Renewable Energy

The goal of this research is to develop a methodology and computational tool that will help us design power systems that are more secure and reliable. In this thesis, we focus on identifying transmission line and reactive power resource reinforcements. Our study investigates both traditional networks and micro-grids that incorporate renewable energy sources like solar panels and batteries. The methodology is based on carrying out a DC optimal power flow (DC-OPF) at the time of peak demand, first on the base-case when all lines are available and next on a series of line outages, one at a time, to test the ability of the system to transmit real power from sources to load centers. Throughout the analysis, fictitious generators are installed at load nodes to represent load-sheds that may be needed in case lines are at their limits and no feasible solution is obtained. When fictitious generators are used, this is either due to a shortage of generation or to a transmission line limitation. If generation is less than demand plus spinning reserve, then it is concluded that the system needs generation reinforcement, which then added at the candidate nodes with the highest local marginal price (LMP). However, if the system has enough generation, then it is concluded that line reinforcements are needed. The line that is selected for reinforcement is the one that is observed to be at its limits when using a fictitious generator. Once the network is deemed adequate in terms of active power transmission, we analyze its base-case, i.e. when all lines are available, using an AC-OPF system, again at peak demand time throughout representative weeks of the year to determine its ability to supply the reactive power demands. If reactive power sources are not sufficient, then static-var-compensation (SVC) systems are added at nodes in a way to minimize the cost of operation.

Our methodology is also applicable for micro-grid systems that entail renewable energy sources (e.g. PV panels) and storage units (e.g. batteries). However, the analysis of micro-grids with renewable energy sources requires identifying the specific hour that is most crucial, which varies depending on the characteristics of the renewable sources and storage sizes. In this case we need to study the system over the different seasons at several hours of the day and select the time at which the system is mostly stressed. Here several options are available for renewable energy sources and storage placement and sizes. The transmission reinforcement study will be carried out on several alternatives and the design to be implemented is the one that leads to a minimum levelized cost of electricity (LCOE) that include capital and operating costs throughout one year of operation. The computational tool that we have developed uses MATPOWER to carry out DC-OPF and AC-OPF analyses and is illustrated on the IEEE 5-bus, 30-bus, and 118-bus systems. We made adjustments to the 30-bus and estimated the transmission lines and transformers' ratings of the 118-bus systems. By implementing these simulations, we verify the accuracy and effectiveness of our methodology.

TABLE OF CONTENTS

ACKNOWLEDGEMENTS 1

ABSTRACT 2

ILLUSTRATIONS 5

TABLES 6

ABBREVIATIONS 8

VARIABLES 9

INTRODUCTION 11

A. Motivation 11

B. Literature Review 12

C. Contribution of this Research 23

D. Research Tools 24

METHODOLOGY 25

A. Optimal Power Flow 25

1. AC-Optimal Power Flow 25
2. DC-Optimal power flow 27

B. Reinforcement Methodology 29

1. Transmission Line Outage 29
2. Reactive Power Reinforcement 33
3. Critical Hour 37

C. Grid Adjustments 41
1. Transmission Line Calculation 41
2. Transformer Calculation 43
2. Generator Calculation 43
D. Calculation 45
RESULTS 46
A. Case Study: 5-Bus System 47
1. 5-Bus Classical Grid Study 47
2. 5-Bus Micro-Grid with Renewable Energy 51
B. Case Study: Younine 18-Bus System 56
C. Case Study: IEEE 30-Bus System 60
D. Case Study: IEEE 118-Bus System 69
CONCLUSION & FUTURE WORK 77
APPENDIX 79
REFERENCES 92

ILLUSTRATIONS

Figure

1. Transmission Line Outage Flow Chart 33
2. AC-OPF Flow Chart 36
3. Younine 18-Bus System 38
4. Transmission performance loading Index Design 1 39
5. Transmission Line Loading Mode Design 1 40
6. Load-ability in per-unit of SIL 42
7. Representation of Power Triangle 44
8. Load Profile 46
9. 5-Bus Microgrid 48
10. 5-Bus Design 1 active flow versus time 56
11. The Younine 18-Bus System 56
12. IEEE 30-Bus Grid 61
13. IEEE 30-Bus Load Flow versus Time 65
14. IEEE 30-Bus Load Flow versus Time (50% Demand Increase) 68
15. IEEE 118-Bus System 69
16. IEEE 118-Bus active demand versus time 73
17. IEEE 118-Bus active demand versus time (50% Demand) 74

TABLES

Table

1. PV and Batteries Sizing and Location 5-Bus System 39
2. Cost Values 46
3. 5-Bus Node Data 48
4. 5-Bus Generator Data 48
5. 5-Bus Transmission Data 48
6. 5-Bus Node Results 49
7. 5-Bus Branch Result 49
8. 5-Bus Data at 40% Demand Increase 50
9. 5-Bus Node Results at 40% Demand Increase 50
10. 5-Bus Branch Result at 40% Demand Increase 51
11. 5-Bus Nodal Data with Renewable Energy (Design 1) 52
12. 5-Bus Transmission Line Flow with Renewable Energy (Design 1) 52
13. 5-Bus Nodal Data with Renewable Energy (Design 3) 53
14. 5-Bus Transmission Line Flow with Renewable Energy (Design 3) 53
15. 5-Bus Nodal Data with Renewable Energy (Design 4) 54
16. 5-Bus Transmission Line Flow with Renewable Energy (Design 4) 54
17. 5-Bus Results AC-OPF 55
18. 18-Bus Node Data 57
19. 18-Bus Generator Data 57
20. 18-Bus Transmission Data 58
21. Top 20 Designs of the Younine 18-Bus System 59
22. Younine 18-Bus Results AC-OPF 59
23. SVC Placement and Sizes (MVAr) for Younine 18-Bus System 60
24. IEEE 30-Bus Node Data 62
25. IEEE 30-Bus Generator Data 62
26. IEEE 30-Bus Transmission Data 63

27. IEEE 30-Bus Summary Table 64
28. IEEE 30-Bus SVC Placement and Sizes 64
29. IEEE 30-Bus Node Results (50% Demand Increase) 66
30. IEEE 30-Bus Transmission Line Results (50% Demand Increase) 67
31. 30-Bus Summary Table with SVC (50% Demand Increase) 68
32. 118-Bus Summary Table with SVC (Base Demand) 71
33. 118-Bus Summary Table with SVC (50% Demand Increase) 74
34. IEEE 118-Bus SVC Placements and Sizes (50% Demand) 75
35. Computer Timing of Different Studies 76

ABBREVIATIONS

AC	Alternating current
AC-OPF	AC- Optimal power flow
BESS	Battery Energy Storage System
CAPEX	Capital Expenditure
DOD	Depth of Discharge
DC	Direct current
DC-OPF	DC-Optimal power flow
DG	Diesel generator
FACTS	Flexible AC Transmission System
LCOE	Levelized Cost of electricity
MIPS	MATPOWER Interior Point solver
OO	Ordinal Optimization
OPEX	Operating Expenses
PU	Per Unit
PV	Photovoltaic
SOC	State of Charge
SI	Surge Impedance
SIL	Surge Impedance Loading
SVC	Static Var Compensator
UPFC	Unified Power Flow Controller
CPF	Continuation Power Flow
UC	Unit Commitment
STATCOM	Static Synchronous Compensator
DRs	Distributed Resources
PWM	Pulse Width Modulation
ESS	Energy Storage System
CP	Capacitor Placement
NR	Network Reconfiguration
FCHEV	Fuel Cell hybrid Electric Vehicles
DP	Dynamic Programming
PSO	Particle Swarm Optimization
EP	Evolutionary Programming
GA	Genetic Algorithm
LDS	Low Discrepancy Sequences
SNTO	Sequential Number Theoretic Optimization
CA	Contingency Analysis
SSA	Static Security Assessment
HPC	High Performance Computing
FDLF	Fast Decoupled Load Flow
TNEP	Transmission Network Expansion Planning
ACO	Ant Colony optimization
MILP	Mixed Integer Linear Programming

VARIABLES

θ	Phase angle
V_m	Voltage magnitude
P_g	Active power from a generator
Q_g	Reactive power from a generator
f_P^i	Active power cost function
f_Q^i	Reactive power cost function
P_i	Active power on a bus
P_d	Demand active power
Q_i	Reactive power on a bus
Q_d	Demand reactive power
F_f	Transmission line flow from a node
F_t	Transmission line flow to a node
F_{max}	Maximum transmission line capacity
V_i	Voltage at a node i
C^T	Cost of operation of fictitious generator
R	Vector of nodal fictitious generator
B_f	Branch to bus admittance matrix
B	Nodal admittance matrix
n_g	Number of energy sources
Z_{base}	Base impedance
S_{base}	Base power
SI_{pu}	Surge impedance per unit
X_L	Transmission line inductance
Y_c	Transmission line susceptance
SI_Ω	Surge impedance in ohm
C_{BD}	Battery degradation cost
I_{BT}	Battery investment cost
A_{BT}	Battery annuity
L_{BT}	Expected battery lifetime operation
N_{BT}	Number of cycles of a battery
η_{inv}	Inverter efficiency
η_{Dis}	Battery discharge efficiency
η_{Cha}	Battery charging efficiency
E_{BT}	Energy of Battery
m_{CO_2}	Mass of CO_2 emitted when burning one liter of fuel
HR	Heat rate
HV	Heating value
E_G	Energy from Generator
M_{CO_2}	Total mass of CO_2 emitted from generators
TC_{PV}	Total cost (Capex and Opex) for PV
F_C	Fuel cost

E_{DG}	Energy from diesel generator
$F_{p/L}$	Fuel price per liter
S_T	Transformer apparent power
$\cos\varphi$	Power factor

CHAPTER I

INTRODUCTION

A. Motivation

In the face of increasing energy demands and environmental concerns, the conventional central grid framework is transitioning towards decentralized and sustainable alternatives. This has led to the concept of microgrids, a localized energy distribution system capable of generating, storing, and managing energy resources autonomously. Microgrids are dynamic embodiments of localized power generation and distribution, with solar energy integration being a crucial aspect. The integration of solar energy into microgrid systems not only helps reduce carbon emissions and reliance on traditional fossil fuels but also provides residents with a renewable and sustainable source of power that minimizes electricity costs. Microgrids' advancing technology presents opportunities to expand these systems to accommodate larger populations or even entire cities, potentially transforming our understanding of energy distribution. However, managing the variability of solar input and seamlessly integrating it into the microgrid's energy mix is a challenge.

Minimizing emissions from conventional generators is another critical concern within microgrid operations. Storage batteries offer a means to store surplus energy during low-demand periods, reducing reliance on generators during peak consumption. Combining battery technology with solar energy can reduce emissions and enhance energy efficiency. Reactive power management is a crucial consideration, with effective control strategies influencing microgrid efficiency and stability. Transmission lines are vital conduits binding microgrid components together, with optimization techniques

aimed at minimizing energy loss and voltage fluctuations taking center stage. As a result, transmission lines are critical to the grid's operation.

The increase in generation and demand necessitates the analysis and planning of transmission lines to assess their performance and reliability. Applying an outage methodology to our grid or microgrid to perform this analysis and evaluate the system performance will lead to a more reliable and optimal connection.

The integration of solar power offers a promising solution for a sustainable energy future. While there are challenges in managing solar variability and optimizing grid stability, battery storage, reactive power control, and transmission line capabilities to manage these variables are paving the way for robust and efficient microgrids. By analyzing and planning these systems using outage methodologies, we can ensure reliable and optimal energy distribution, transforming how we generate and deliver power.

B. Literature Review

Fi1lipe et al. [1] present simulation results of a microgrid that includes a photovoltaic (PV) generation system, batteries, support generators, and a distribution system load. In general, microgrids are built to effectively integrate energy storage and renewable energy sources for distributed power generation. The main goal of this research is to create a solid control system that can manage energy resources and consumer loads within intelligent microgrids, making it easier to integrate distributed generation efficiently. The suggested control structure enables the PV system to extract the maximum amount of power, meet the demands of the loads, and maintain a balanced power flow to guarantee transient stability within the microgrid.

Flexible Alternating Current Transmission Systems (FACTS) technology, according to Vjollca et al. [2], allows for effective control of power flow, enhancing stability and power-handling capacity. They accomplished this by injecting reactive power through electronically controlled power elements that can be connected to the power lines either in series or in parallel. A sophisticated power electronic device that can control local bus voltage and optimize power flows is the (UPFC). Using simulations in a MATLAB/Simulink environment, the paper examines how UPFC and FACTS devices are used on a 400 kV transmission line. The study's conclusions highlight how well the UPFC controls both active and reactive power flow while minimizing line outages.

Venkata Ramesh et al. [3] suggest using a STATCOM and a fixed capacitor bank for reactive compensation in a grid-connected solar PV array system. To assess the system's performance under various solar PV array irradiance and reactive load power conditions, they provide an overview of the design calculations and simulation of the system using MATLAB and Simulink. The study illustrates the efficient reactive power management of the grid-connected solar PV array system using STATCOM and a fixed capacitor bank. The simulation results show that STATCOM performs better in this situation for compensating reactive power than fixed capacitor banks.

Ya Guo et al. [4] present a novel power flow control and optimization method for microgrids in grid-connected mode. It explores factors such as electricity cost, battery degradation cost, and battery charging/discharging efficiencies. A universal normalized mathematical relation is developed and verified at critical operation points between all costs. Based on a dynamic programming algorithm, the proposed optimization approach can find the global optimal solution for microgrid power flow dispatch for different electricity trading and battery storage conditions. The research also provides a normalized

universal mathematical relation between different costs, which is useful for microgrid end-users to estimate the necessity and sizing of their battery storage. Simulation results verify the effectiveness of the proposed method and the derived relation, demonstrating the robustness of the approach to deal with forecast PV error. The experimental results validate the simulations with high compliance.

Bilal Eid et al. [5] focused on addressing power quality issues associated with integrating Photovoltaic (PV) systems as distributed resources (DRs) into the utility grid. The main concerns are reactive power compensation and voltage regulation. The connection between the PV source (DC) and the utility grid involves an inverter, and the paper utilizes the Pulse Width Modulation (PWM) technique to optimize the DC link voltage and achieve reactive power compensation at the point of common coupling (PCC). MATLAB/Simulink simulations demonstrate the effectiveness of the proposed controller in managing these power quality challenges. The controller adjusts inverter switching times to stabilize DC voltage, synchronize inverter output with the grid, and minimize reactive power at the PCC. The simulation results show the controller's ability to achieve these objectives regardless of power source intermittent and load disturbances.

Parvathy. S et al. [6] address the intermittent nature of renewable energy generation and its impact on the reliable operation of microgrids, crucial components of future smart grids. The paper proposes energy cooperation among microgrids as a solution, in addition to commonly adopted approaches like energy storage systems (ESS) and supplementary fuel generators. The study focuses on two cooperative microgrids, each equipped with individual renewable energy generators and ESS. The research includes an offline optimization to manage energy efficiently when renewable energy generation and load amounts are known in advance. It explores the effects of microgrids'

energy cooperation and ESS utilization on reducing total energy costs. The paper also proposes online algorithms for real-time energy management based on the offline optimization results, showcasing their effectiveness through simulations. Furthermore, the paper suggests extending these algorithms to scenarios involving more than two microgrids through a clustering approach. Overall, the proposed approaches demonstrate promising performance and low complexity, highlighting their practical viability in managing cooperative microgrids with intermittent renewable energy profiles.

Jabr et al. [7] addresses the Capacitor Placement (CP) problem, it is a complex nonlinear mixed-integer optimization problem involving the placement and number of capacitors in a distribution network. The aim is to minimize power losses effectively using CP and network reconfiguration (NR) through intelligent soft computing approaches. The paper proposes employing ordinal optimization (OO), leveraging order comparison and goal softening to enhance computational efficiency. The study applies OO to 33 and 69 bus systems, comparing the results with other recent methods. The reduction in losses achieved using OO for CP and NR demonstrates its effectiveness and prompts further exploration. The paper outlines the OO technique for optimal CP and NR, utilizing sensitivity analysis to select the most effective candidate buses and a two-stage OO approach to optimize the capacitor values. The results indicate superior power loss reduction compared to other published methods, encouraging further research on the OO method for CP. Additionally, integrating NR with CP proves to be a potent approach, surpassing the individual power loss reduction achieved by CP or NR alone.

Karaki et al. [8] introduces an optimal design methodology for fuel cell hybrid electric vehicles (FCHEV) using ordinal optimization (OO) and dynamic programming (DP). It aims to minimize investment and operational costs by determining appropriate

sizes for components like the hydrogen tank, fuel cell, battery, and motor based on specified car range, road type, and gradeability. DP simulates vehicle operation for various component sizes and driving cycles, providing total vehicle cost per year. OO efficiently ranks and selects a set of "good enough" designs through two models, allowing for cost-effective FCHEV power unit designs. The approach considers various design specifications and highlights the economic advantage of hybrid designs incorporating energy storage like batteries.

A. Dhaneria et al. [9] addresses the issue of increased reactive power demand from the grid due to the rising deployment of renewable Distributed Energy Resources (DERs) like solar. It proposes enhancing grid-tied solar inverters to supply reactive power in addition to active power, thereby reducing the grid's reactive power supply burden and enhancing power quality. The paper discusses various methods for PV inverters to absorb and inject reactive power. It presents simulation results for different static reactive power compensation control strategies, highlighting the effectiveness of these approaches. The study emphasizes the importance of integrating reactive power compensation capabilities into solar inverters to enhance system utilization, especially during periods of limited solar irradiance.

H. Barout et al. [10] conducts a comprehensive analysis of constrained optimal power flow for reactive power planning, switching, and dispatch in power systems. It establishes the minimum feasible line limits achievable with appropriate reactive power compensation to enhance transmission line security. The study segregates total system transmission losses into real power flow-induced losses and reactive power flow-induced losses, examining their dependence on reactive power flow. The impact of reactive power support on these loss components is assessed, offering valuable insights into the variation

of transmission loss components during different load conditions and power-factor variations. The research identifies buses requiring sustained reactive power support and proposes a comprehensive reactive support plan for the system. It demonstrates that executing an optimal power flow (OPF) program with cost optimization significantly reduces the overall system operating cost, albeit with a slight increase in system losses. The paper verifies the effectiveness of the proposed reactive power plan using loss minimization as an objective function and shows that adequate reactive power support allows for more stringent transmission congestion limits. Additionally, the study establishes a new relationship between the two loss components and system load variation for both objective functions, shedding light on the effect of reactive compensation on these relationships. The analysis underscores the importance of reactive power support in minimizing losses and enhancing system performance.

S. Kahourzade et al. [11] present a comprehensive comparison of three different population-based algorithms, namely particle swarm optimization (PSO), evolutionary programming (EP), and genetic algorithm (GA), for solving the multi-objective optimal power flow (OPF) problem. The study evaluates the performance of these algorithms in optimizing single-objective and multi-objective functions, including cost, active power loss, voltage stability index, and emission. The research focuses on the necessity of a multi-objective OPF study due to the unattractive characteristics of cost based OPF, which include loss, voltage profile, and emission. The study uses the Pareto optimal method to create a set of solutions for each algorithm and applies a fuzzy decision-based mechanism to select the best solution from the Pareto set. To validate the effectiveness of the proposed methods, the algorithms are tested on an IEEE 30-bus test system. The results indicate that EP offers the best price in most cases compared to PSO and GA. The

study emphasizes the importance of considering secondary criteria in addition to individual optimizations, highlighting the interrelated nature of the objective functions.

A. Alabduljabbar et al. [12] have developed an optimization algorithm for the optimal placement of Flexible AC Transmission System (FACTS) devices in a power network to reduce generation costs. The study uses Low Discrepancy Sequences (LDS) to determine the optimal number, size, type, and location of FACTS devices, considering both active and reactive power generation costs. The Sequential Number-Theoretic Optimization (SNTO) algorithm is introduced as part of the optimization process. The study uses mathematical models for steady-state behavior of FACTS devices. The IEEE New England Test System is used as the test network. This paper highlights the effectiveness of the LDS-based optimization approach for FACTS device placement in reducing generation costs. The study provides valuable insights into the optimal utilization of FACTS devices for power systems.

Panda, P.C. et al. [13] explores the utilization of Static Var Compensators (SVC), a type of Flexible AC Transmission System (FACTS) device, for improving voltage stability and minimizing losses in a nine-bus power system. Through load flow analysis and the Newton-Raphson method, the study compares the performance of the uncompensated system with the SVC compensated system, identifying bus 4 as the optimal location for SVC placement due to its effect on minimal voltage variation and reduced losses. Optimality is obtained by changing the position of SVC from bus 1 to bus 9, and the results are compared according to voltage magnitude and loss reduction. The load flow indicates that adding an SVC to bus 4 enhanced the voltage stability and reduced the losses. The research underscores the significance of FACTS controllers

in enhancing power system flexibility and reliability, emphasizing the need for optimal placement to achieve maximum benefits in terms of voltage stability and loss reduction.

P.S.V. Prabhakar et al. [14] discovered that contingency analysis (CA) is critical for static security assessment (SSA) in power systems, predicting operating states under various outages, including generators, transmission lines, and transformers. This needs a lot of load flow analysis to find out the bus voltages, injections, and line flows for every possible outage. This calls for efficient system modeling, parallel programming, and high-performance computing (HPC). This paper presents an N-1-1 contingency analysis using Fast Decoupled Load Flow (FDLF), focusing on reducing computational complexity in large power systems. In addition to the usage of sensitivity analysis for choosing the lines and generators to apply outages on them. The method, demonstrated on IEEE 14 and 118 bus systems, uses outage distribution factors and performance indices to screen and rank contingencies. The study highlights a computationally efficient SSA method using state-of-the-art HPC for parallel and distributed computing.

According to Kumar, Uday et al. [15], addressing contingencies from unplanned or planned line outages that lead to system overloads or abnormal voltages is a critical aspect of modern power system security assessment. Despite the development of various methods, the process remains inefficient due to the constraint of computation time. Utilities need tools to predict grid stability and reliability in real time. A power system is considered secure if it operates within tolerable limits before and after a contingency. Contingency ranking estimates the impact of contingencies without solving the power network, but existing methods suffer from masking effects and slow execution. This paper presents an exact and precise method for contingency ranking, considering both apparent power overloading and voltage violations. Using the 1P1Q solution to find post-

contingency voltages and power flows, the method is simulated on IEEE-14 and IEEE-30 bus test systems in MATLAB. The results show that the indices are calculated to measure the severity of possible line outage contingencies, with the highest values indicating the most severe outages. This method is accurate, precise, and fast enough for security analysis in complex power systems.

Maghouli et al. [16] presents a static transmission line expansion methodology using the multi-objective optimization framework, taking into consideration investment cost, reliability and congestion cost. NSGA II genetic based algorithm with the selection of a random initial population and fuzzy decision making analysis are used to solve the nonconvex and mixed integer optimization problems. This methodology is used on the IEEE-24 bus test system and also applied to the Iranian national for the 400-KV transmission grid system. The proposed methodology allows for a cost benefit approach that handles stakeholders preferences and incorporates static security analysis as a first step in order to provide more optimal solution and flexibility in the planning process.

A.Mahmoud Abadi et al.[17] stated a transmission network expansion planning (TNEP) and a reactive power planning methodology which is a complex issue in a new restricted electricity markets. This paper presents a combinatorial mathematical model to solve the transmission expansion and reactive power planning. The model uses a mixed integer nonlinear problem with an objective function that includes the investment and production cost of the expanded circuit as well considering the load curtailment penalty payments. A real genetic algorithm is employed to obtain a quality solution to the complex problem. An interior point method is applied to solve the optimization problem of the reactive placement and sizing. The model is tested on two well-known systems, Garver and IEEE 24-bus, and the results show significant performance and robustness.

The main contribution of this model is to handle the transmission expansion and reactive power planning simultaneously in deregulated markets, that achieve an optimal solution compared to traditional models.

R. Alvarez et al. [18] presents a novel meta-heuristic multi-year transmission network expansion planning (TNEP) model based on ant colony optimization (ACO) for the dynamic transmission line expansion problem. This model considers flexible expansion options, voltage uprating, and adding series compensation. This model was tested on Garver's 6-bus test system and on a modified version of the IEEE-118 bus system. The results showed excellent performance in terms of solution quality and computational times compared to traditional mixed integer linear programming (MILP) approach. This paper include line upgrading options within the multi-year transmission expansion that brings significant benefits such as reducing total investment and congestion cost of the system. This model extends beyond the addressed case studies presented in this paper, allowing for evaluation of further expansion options. This novel model offers a more efficient and cost-effective approach for transmission line expansion.

Buygi et al. [19] presents a new market-based approach for transmission planning in deregulated environments. It introduces a probabilistic tool called probabilistic locational marginal prices for computing the probability density function of nodal prices, that defines a new marked based criteria for transmission expansion planning. This approach provides nondiscriminatory access to cheap generation for all consumers that consider all random and nonrandom power system uncertainties. This methodology was applied to the IEEE 30-bus system, and it demonstrated the effectiveness of the market-based criteria in single and multiple cases. This approach aims to facilitate competition

and provide nondiscriminatory access to cheap generation by providing a flat price throughout the network.

Mahdavi et al. [20] presents a comprehensive review and classification of significant work on transmission network expansion planning, focusing on literature framework, including traditional approaches, transmission planning including maintenance, uncertainties in generation and demand, reliability, electricity market, energy storage, and risk management. This paper categorizes transmission network expansion into four major classifications: models, solution methods, case studies, and innovations. This categorization indicated the most researches have focused on static solutions to the transmission expansion problem, although some have used dynamic approach. Metaheuristics is the most commonly used solution method due to large scale combinatorial feature of the transmission expansion problem. However, the DC power flow is the most common representation of the transmission network within transmission line expansion approaches due to the high complexity associated with the AC representation.

R.P.O'Neill et al. [21] presents a new modeling approach for inter-regional planning and investment in a competitive environment. This approach incorporates detailed generator topology and operational aspects for production cost planning models into a large framework to find optimal sets of transmission expansion projects. The model is a two-stage, mixed integer, multi-period, N-1 reliable model with investment, unit commitment, and transmission switching. The model may be computationally intractable without judicious modeling aggregation. The paper presents a process for planning, and

a formulated transmission planning model that introduces sensitivity analysis techniques and presents several approaches to the allocation of transmission costs.

Latorre et al. [22] presents a transmission planning methodology that focuses on the most interesting models found in international technical literature. The classification of publications considers solution methods on treatment of planning horizon. The paper presents a classified list of major publications on transmission expansion (synthesis models), which are essential guidelines for those entering the research field. However, these models have limitations, such as not considering ohmic losses, neglecting demand changes, not considering realistic scenarios, and not considering multiple contingencies. They also neglect alternative options such as rearranging or upgrading the grid. Mathematical optimization models have also limitations such as the usage of the DC load flow that eliminates multiple factors. The heuristic model has proven to be a viable alternative for solving real-world transmission planning problems.

C. Contribution of this Research

This thesis focuses on analyzing both grid and microgrid systems with renewable storage, blending multiple innovative ideas. First, we developed a tool that analyzes transmission line performance by conducting a transmission line outage analysis across of the grid and applying a DC-OPF for each line outage. Unlike previous studies that typically prefer sensitivity analysis to select a limited number of branches for contingency analysis, our approach ensures a comprehensive evaluation of grid robustness.

After confirming the reliability of our grid on the transmission side, we aim to minimize operational costs and losses. Were our main objective is to minimized the usage of active power. This is achieved through the use of AC-OPF, applied over an entire year

or the usage of representative weeks of the year that gives a great demonstration to determine the optimal location and size of the SVC. The application of AC-OPF is more accurate than traditional load flow analysis or the Newton-Raphson method as it optimally implements economic load dispatch with line constraints. Furthermore, our methodology for optimizing the SVC is more precise than simply adding an SVC at one node and monitoring grid performance, which might be feasible for a 9-bus system but becomes impractically complex for a 118-bus system.

The integration of renewable energy not only reduces the overall system-operation cost, but also improves its efficiency. We apply both methodologies DC-OPF for the line outage analysis and AC-OPF reactive support analysis to microgrids with renewable energy elements, demonstrating how the inclusion of renewable sources enhances the grid's efficiency and security. Our approach provides a robust framework for optimizing both grid and microgrid performance, ensuring reliability and cost-effectiveness in systems incorporating renewable energy.

D. Research Tools

To carry out this research, we have used MATLAB, created by MathWorks, which we have used as a tool for manipulating matrices, graphing functions, data analysis, and implementing algorithms. We have also used MATPOWER, which is a set of free, open-source MATLAB M-files to simulate the operation of power systems in a steady state. We have used the DC optimal power flow (DC-OPF) to simulate the system under outage analysis, and used the AC-OPF the reactive power requirements of a system following the transmission line reinforcement.

CHAPTER II

METHODOLOGY

A. Optimal Power Flow

1. AC-Optimal Power Flow

Electric power systems, which consist of interconnected generators, transmission lines, transformers, and loads, have a vital impact on our everyday existence. They provide a consistent supply of electricity to our homes, commercial establishments, and industrial facilities. However, at the heart of this process lies an intricate obstacle, namely the AC Optimal Power Flow technique. The AC-OPF is a mathematical methodology that necessitates the use of non-linear optimization techniques. When employing the AC-OPF, our goal is to determine the check the final operation of the studied system and determine its reactive power requirements. The objective in this formulation is to minimize the cost of fossil fuel generators, while maintaining voltage stability through the use of reactive power capabilities of existing generators, PV and battery inverters when available, and if need be the use of static-VAr-compensators (SVC). We are simulating the preference of system operators to improve performance in terms of reactive power by first using available resources and if need be to add the SVC. The AC-OPF problem is subject to numerous constraints, consisting of the following:

- **Power balance constraints:** To ensure that the amount of power generated is sufficient to meet both the power demand and associated power losses.
- **Generator constraints**: To adhere to the operating limitations of generators, including their capacity in terms of active and reactive power.
- **Voltage constraints:** To ensure that voltage levels remain within the specified operating limits of ±5% of nominal value.

- **Transmission line limits**: To ensure that the current passing through transmission lines does not exceed their maximum rated limit.

We have used the AC-OPF method to analyze the grid at different hours of operation. By running these simulations, we aim to determine whether the grid requires additional reactive power support or if it can effectively manage its reactive power demands using the existing generator reactive sources. The optimization vector x for the AC-OPF problem consists of voltage angles Θ and magnitudes V_m vectors, each of size n_b, and of vectors of real and reactive power injections P_g and Q_g, also each of size n_b.

$$x = \begin{bmatrix} \Theta \\ V_m \\ P_g \\ Q_g \end{bmatrix}$$

The optimal power flow objective function is minimizing the cost function $f(x)$ where it is the summation of individual polynomial cost functions f_P^i and f_Q^i of active and reactive powers, respectively:

$$f(P_g, Q_g) = min \sum_{i=1}^{n_g} f_p^i(p_g^i) + f_Q^i(q_g^i) \tag{1}$$

This objective function is subjected to equality and inequality:

$$P_{bus}(\Theta, V_m) + P_d - P_g = 0 \tag{2}$$

$$Q_{bus}(\Theta, V_m) + Q_d - Q_g = 0 \tag{3}$$

$$\left|F_f(\Theta, V_m) - F_{max}\right| \leq 0 \tag{4}$$

$$\left|F_t(\Theta, V_m) - F_{max}\right| \leq 0 \tag{5}$$

$$\mathrm{v}_i^{min} \leq \mathrm{v}_i \leq v_i^{max} \quad (6)$$

$$\Theta_i^{min} \leq \Theta_i \leq \Theta_i^{max} \quad (7)$$

$$p_g^{i,min} \leq p_g^i \leq p_g^{i,max} \quad (8)$$

$$q_g^{i,min} \leq q_g^i \leq q_g^{i,max} \quad (9)$$

2. DC-Optimal power flow

DC-OPF is a crucial tool in the field of electrical power systems, which is a simplified version of the AC-OPF where the power flow equations are expressed by using a linearized form which makes the simulation of the DC-OPF much faster than the AC-OPF. Despite its simplifications, the DC power flow model provides good approximations for numerous practical applications. The DC-OPF formulation is based on a number of critical assumptions, which simplify the problem without losing considerably on accuracy.

- **Linearization of Power Flow Equations**: The AC-OPF equations are complex and nonlinear. DC-OPF linearizes these equations by assuming small angle differences between buses of a transmission line, which simplifies the computation and makes the problem more manageable.
- **Neglect of Reactive Power:** DC-OPF concentrates exclusively on active power (actual power), disregarding reactive power components. This reduces the complexity of the problem, allowing for quicker computation times.
- **Constant Voltage Magnitudes:** DC-OPF presupposes that the voltage magnitudes are consistent and correspond to their nominal values, resulting in minimal voltage fluctuations.

- **Fast simulation:** The DC-OPF is faster than the AC-OPF due to neglecting line resistance, assuming that all branch resistances are zero. The DC-OPF assumes a constant voltage magnitude, in which all voltage magnitudes at nodes remain constant and match the nominal voltage. This modeling enables the simulation to be linearized and simplified, as well as speeding up computation.

We chose to include DC-OPF in our code to analyze transmission line outages and generator reinforcement because of its numerous advantages and ability to effectively manage a diverse array of system scenarios with optimal power flow. This methodology ensures the system's dependable and cost-effective operation, making it an "optimal" choice for rapidly improving power distribution in complex power networks.

To solve the standard optimal power flow problem, you must find the set of voltages and flows in a network that match a certain pattern of production, load, limits, and constraints. MATPOWER has solvers for DC-OPF power flow problems. To solve this type of problem, you need to solve a set of equations. In this section, we will discuss the DC-OPF objective function as well as the equality and inequality constraints.

The optimization vector x for the DC-OPF problem consists of $n_b \times 1$ vectors of voltage angles Θ and real power injections P_g

$$x = \begin{bmatrix} \Theta \\ P_g \end{bmatrix} \tag{10}$$

The optimal power flow objective function is minimizing the cost function $f(x)$ where it is the summation of individual polynomial cost function on the active cost f_P^i and the cost of the load shed $C^T R$.

$$f(P_g) = min \sum_{i=1}^{n_g} f_p^i(p_g^i) + C^T R \tag{11}$$

This objective function is minimized subject to equality and inequality:

$$B_{bus}\Theta + P_d - P_g - R = 0 \tag{12}$$

$$-F_{max} \leq B_f\, \Theta \leq F_{max} \tag{13}$$

$$\Theta_i^{min} \leq \Theta_i \leq \Theta_i^{max} \tag{14}$$

$$P_g^{i,min} \leq P_g^i \leq P_g^{i,max} \tag{15}$$

$$0 \leq R \leq P_d \tag{16}$$

B. Reinforcement Methodology

1. Transmission Line Outage

In power systems, ensuring the network's dependability and stability is of utmost importance. An essential component of this process involves the examination and control of disruptions in transmission lines. An interruption of a transmission line can have substantial consequences for the electrical system, such as excessive loads on the lines, instability in voltage, and, in the most severe situations, blackouts that affect the entire system. Ensuring the system's reliability and minimizing disruptions requires efficient power outage management and comprehensive preparedness for unexpected events.

The transmission line outage analysis entails a series of essential processes aimed at evaluating the consequences of an outage and identifying suitable remedial measures. We will conduct the analysis in our DC-OPF model, facilitating the simulation of diverse situations and understanding the system's response to various eventualities.

Before running the model through the transmission line outage logic, we prepare the case setting and make sure the MATPOWER case's data structure encompasses bus, branch, generator, and generator cost data. We must select a contingency set based on the branch data, which we can extract from our system to ensure continuity without cutting a bus from power. Usually, several protective measures are implemented at substations, thus transformers and buses are well protected from lightning and other external elements that can cause faults. In relation to the generators, we may have a standby generator on our bus for emergency situations, or we may be preparing to add a generator station to this bus in the future. We can incorporate this generator into our data, switch it off, and use it to determine if its placement at this node is beneficial for future planning. Furthermore, we consider the operational cost of the generator that is on standby, even if it is in off status as if it is a generator located on a node that is used only for an emergency situation.

To maintain continuity of solution, we introduce fictitious generators into the system, which are added at load nodes just to avoid infeasibility errors. These fictitious generators have operating costs that represent the social cost of losing electricity at the corresponding node or the cost of an alternative power supply. In principle they may be added at any node, but it is our preference to place them at load nodes. After adding these generators, we will run our case through the DC-OPF model to determine if any fictitious generators are in use. If they are, then we have two cases: either a line might be on the limit, or we have a lack of energy supply to the load due to the increase in demand. If a branch is at its limit, we must reinforce it, rerun the case, and recheck. However, if there is no branch at its limit, we must reinforce the generators. Checking the generation reinforcement set and selecting it is necessary here. This is dependent on the incremental

cost at each node that the DC-OPF can calculate while running. If the incremental cost on all buses is equal, we will turn on any generator from our reinforcement set; if not, we will select the bus with the highest incremental cost with a reinforcement generator and turn it on.

If the case does not require a generator addition, we can address the system throughout the outage logic. Referring to transmission line data and limits, lines are capable of handling loads above their limits for a certain time. Therefore, prior to line removal, all lines limits are increased by 15% to model the relaxing of lime limits in a contingent situation. A contingency set of branches is selected in the structure before running the case. The code will begin by eliminating the branches from the set, executing the case through the DC-OPF, and verifying the use of fictitious generators. Then the same tests are done to decide whether the system requires transmission line reinforcement.

Overall, the outlined procedure for analyzing transmission line outages in the DC-OPF model offers a thorough methodology to guarantee the efficiency and dependability of power networks. By organizing the case settings such as branch data, bus data, generator (PV, battery SVC, diesel if available) sizing and location, load profile, irradiance, temperature and cost data, we can precisely model different contingencies and comprehend the system's reactions. Using fictitious generators makes it easier to resolve infeasibility problems like branch limits or not enough energy, which lets us focus on reinforcing specific branches or generators.

By utilizing incremental cost analysis and strategically activating reinforcement generators, we guarantee the optimization of the system for both present operation and

future planning. The process of preparing the contingency set and systematically eliminating branches, along with a 15% rise in rating limitations, offers a strong and reliable framework for testing and strengthening the network [23]. This rigorous procedure not only reduces the likelihood of power outages and system instability, but it also improves the power system's reliability by ensuring it is well-equipped to handle unexpected disturbances.

In summary, the methodical approach described in this analysis emphasizes the critical importance of proactive power outage management, as well as the need for ongoing assessment and strengthening of the transmission infrastructure. Through testing and strengthening of the system, we can greatly diminish the probability of disruptions and guarantee a steady and dependable power supply.

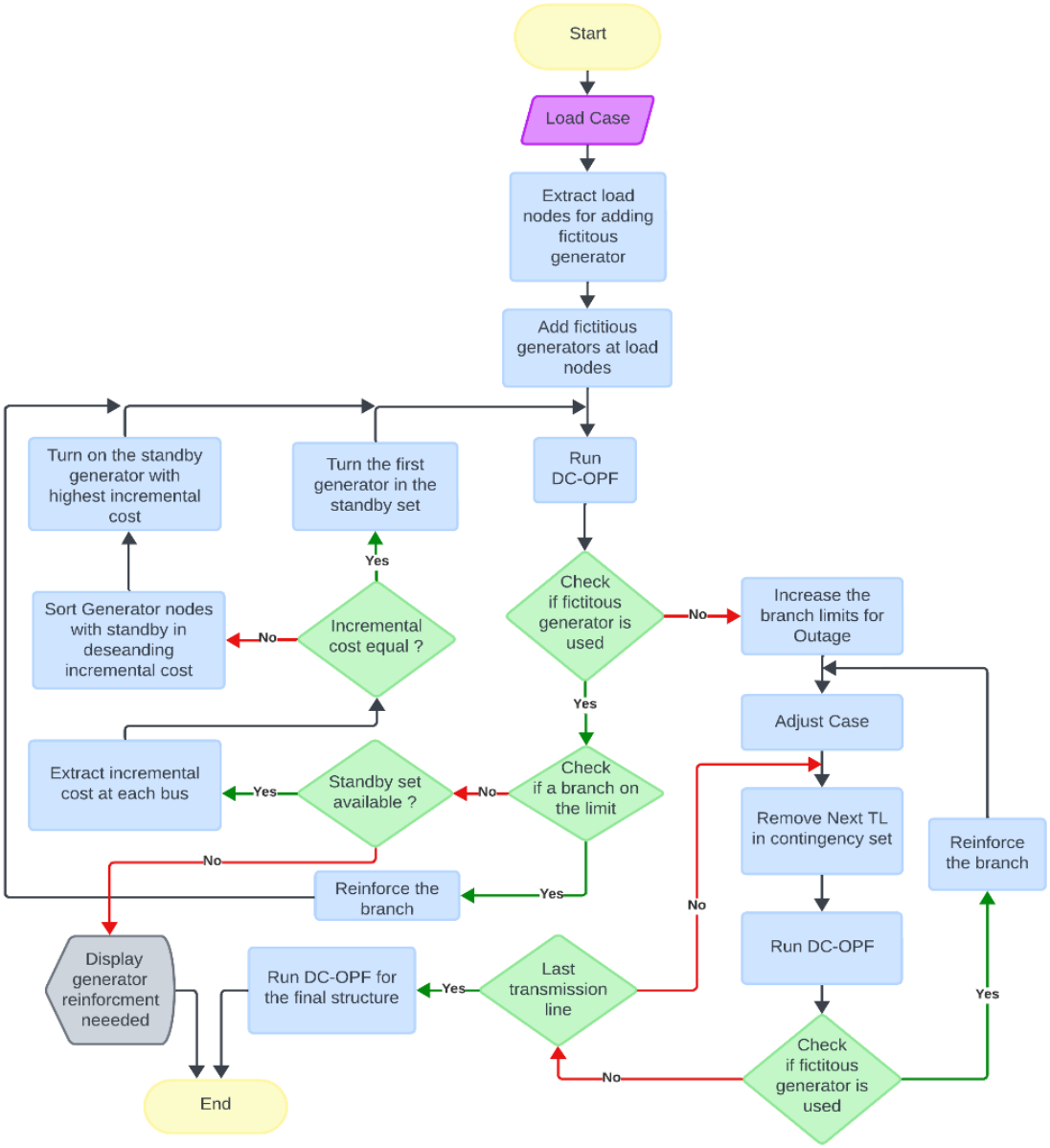

Figure 1: Transmission Line Outage Flow Chart

2. *Reactive Power Reinforcement*

After conducting a thorough line outage analysis for our system, we aim to ensure its capability to operate efficiently in the AC domain. This involves assessing whether the system requires reactive power support to maintain adequate operation. By simulating various outage scenarios, we can identify potential vulnerabilities and determine the

necessary measures to mitigate any adverse impacts on the system's performance. This analysis is critical for optimizing the system's design and ensuring its robust operation under different conditions.

The process starts with the collection of essential data, including the load profile, temperature, irradiance, and other system-specific data such as bus and branch data, and any reinforcement that have been added. We also need to specify design alternatives for the available resources, such as PV, batteries, generators, reinforcement generators, and SVC, taking into account their placement and size. We propose locating SVC's at all nodes in our grid while relaxing their reactive limits thus allowing the AC-OPF to choose the location and the size required this is as a first step for the SVC sizing and placing. Following this, we will calculate the average reactive demand (ARD) per node, then we will compare the maximum value chosen of the SVC usage to 0.01 of ARD, over the interval of analysis; if SVC is smaller 0.01 ARD, then it will be removed from the system as a resource of reactive power.

Then, we set economic data for the available resources, ensuring that we consider the cost implications for active and reactive elements as an operation of the element, in addition to the investment and operational cost of each element introduce in our system.

The next phase involves starting with the initial design. An iterative process begins here, checking if the current design is the last one. If not, we analyze the first hour of the time interval. We extract the solar panel power output for each hour. The system then checks if the solar power at this hour is less than or equal to the demand. If the solar power is less than or equal to the demand, checking the battery's state will be necessary.

If the batteries can meet demand, the generators are in standby. If batteries run low, generators will meet demand.

On the other hand, if solar energy is greater than the demand, this will involve checking if the batteries are at their maximum SOC. If batteries are in their maximum state of charge, then they are on standby; if not, they will be charging. Each hour, we handle the energy distribution, run an AC Optimal Power Flow (AC-OPF) analysis, and store the optimal flow results. We then update the state of charge of the batteries accordingly. We repeat this process for each design and every hour until we reach the final design and time interval.

Finally, we calculate the total system cost, which includes Capex, Opex, total energy, carbon dioxide emission and the LCOE system. The next step involves sorting different designs in ascending order of LCOE. We plot the energy elements and demand to provide a visual representation of the system's performance. This comprehensive analysis concludes the process, identifying the most cost-effective and efficient design.

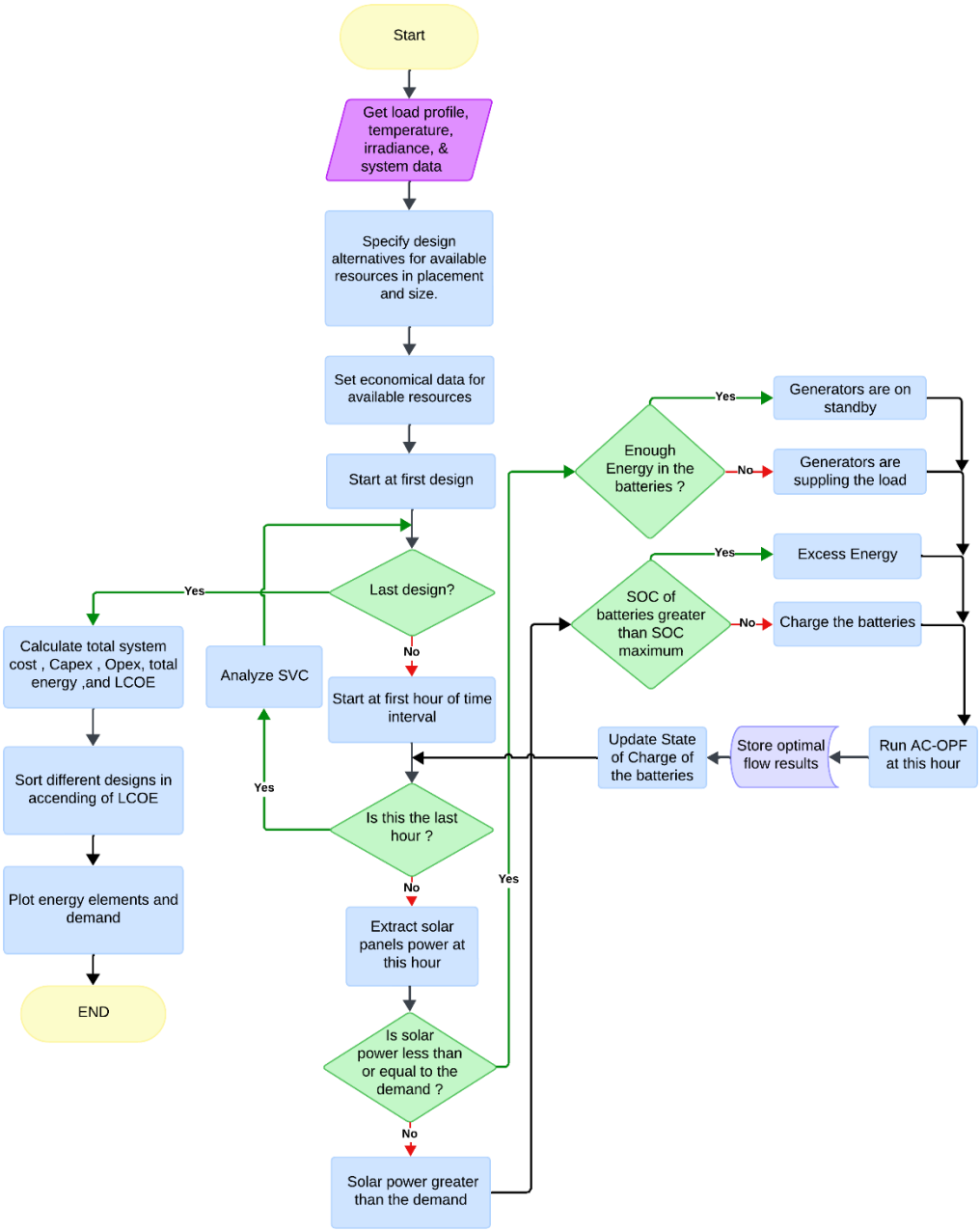

Figure 2: AC-OPF Flow Chart

3. Critical Hour

When we investigated the effects of a transmission line outage on a grid with renewable energy components e.g. (PV & BESS), we found that the grid does not experience its mostly extreme stress during periods of maximum electricity demand, unlike when we examine a traditional grid. This finding suggests that there are several factors that affect grid loading.

There are several variables that influence the grid loading, such as demand, solar irradiance, battery state of charge, grid component positioning, and temperature fluctuations. Understanding the interaction between these factors is critical to obtain a critical hour that is used for maximizing the power grid's durability and efficiency in a variety of operational scenarios. Therefore, we proposed to analyze the transmission line during different seasons, dividing the year into four parts: winter, summer, autumn, and spring. Each of these seasons might have a different critical hour due to the different irradiance levels, temperatures, and demands.

In this thesis, we are using the 5-bus and Younine18-bus systems [24], which incorporate renewable energy components. However, due to the radial nature of the Younine 18-bus system, as shown in Figure 3 implementing a transmission line outage is not possible. Isolating a node from a grid will cause a singular Jacobian matrix that will lead to an infeasible solution. We will illustrate determining the critical hour for each of 8 designs, in a 5-bus micro-grid system [24], by simulating their operation throughout the sampled timeline, and we will use this critical hour for the transmission line outage of each design. Therefore, at each hour of our timeline, we run a DC-OPF, and evaluate the transmission line performance (TLP) index given as follows:

$$TL_h = \sqrt{\sum_{l=1}^{L} (F_l(h) - F_{max})^2} \qquad (18)$$

$$for\ h = 1\ ,2\ ,3\ \ldots\ldots$$

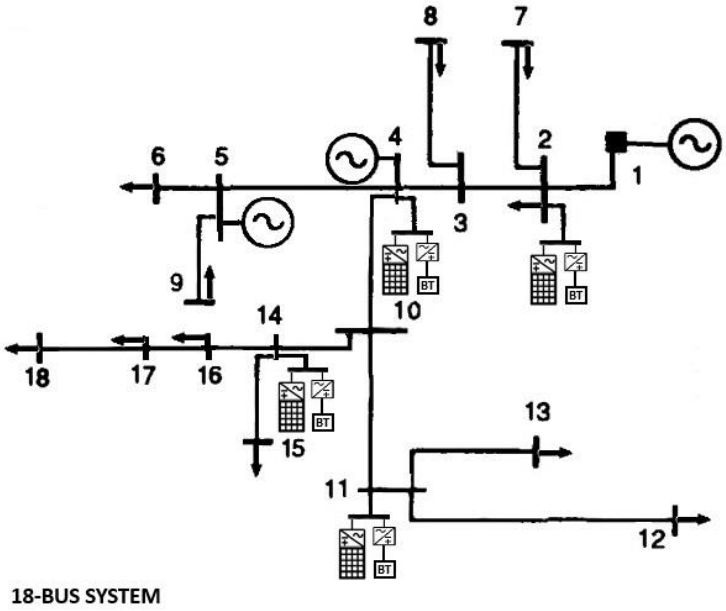

Figure 3: Younine 18-Bus System

Table 1 displays the size and location of the PV and batteries of the selected 8 designs. We will use this example to determine a critical hour for each design, analyze the results, and select the hour to apply the line outage methodology on this microgrid. We run each design for the representative data of the year, and determine the TLP index at each hour, which are shown in Fig. 4 for Design 1.

Table 1: PV and Batteries Sizing and Location 5-Bus System

			Nodes PV (MW)			Nodes BT (MWh)		
Design	PV	BT	1	2	3	1	2	3
1	30	64	15.3	8.7	6.0	1.3	43.5	19.2
2	30	66	15.3	8.7	6.0	2.0	44.2	19.8
3	30	68	15.0	8.7	6.3	2.0	44.9	21.1
4	32	62	15.7	9.0	7.4	1.3	41.5	19.2
5	32	64	16.0	9.3	6.7	1.3	42.9	19.8
6	32	66	16.0	9.6	6.4	1.3	44.2	20.5
7	30	70	15.0	8.7	6.3	2.8	44.8	22.4
8	32	68	15.7	9.6	6.7	2.0	45.0	21.0

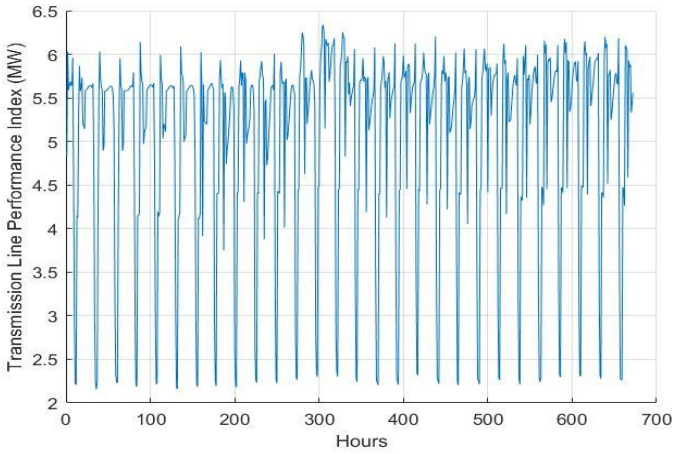

Figure 4: Transmission performance loading Index Design 1

It is clear from Fig. 4 that the critical hours occur at the minimum values of the TLP index. We note that this is occurring at hour 10 of the first day, and hour 34 which is hour 10 of the next day. To make this point clearer, we determined for each design the mode of minimum TLP as shown in Fig. 5 below. Here note that the TLP minimum was predominantly observed at 10:00 AM due to only slight differences in the sizes of PV systems and batteries across designs. Accurate monitoring of the data revealed that after a night of supplying load demands from the batteries, which reached their minimum state of charge by dawn, the solar panels began to generate power. However, with the batteries completely depleted, the solar panels seem to have the capacity to meet the entire demand,

leaving some excess of power available for battery charging. This might seem non-logical due to the placement of the batteries and PV on the same node; however, different PV nodes have different sizes, and this leads to variation in energy production, which leads to charging from node 1 to node 3, for example. This led to multiple nodes contributing power to the load nodes and charging nodes, resulting in high branch loading in the transmission lines.

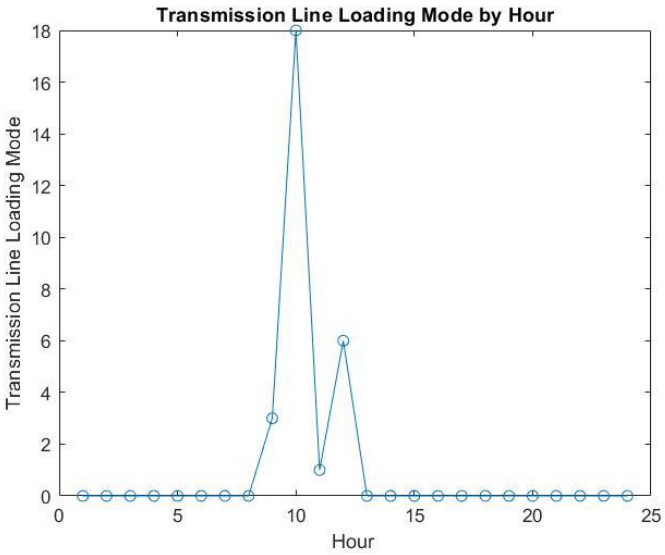

Figure 5: Transmission Line Loading Mode Design 1

After conducting the study, we found that this method may not be the most effective way to determine the critical hour in a system where multiple variables are affecting the transmission line. However, it provided a rather clear understanding of our grid's performance. We demonstrated that in a renewable energy grid, the maximum loading does not occur during peak times but fluctuates due to various factors such as component placement and size, and irradiance levels. This insight is valuable for future grid planning and optimization, where we can work on it and make it more precise by

taking more factors into consideration, solar irradiance, temperature effect, PV and battery placements and sizing to make it more likely to reach optimality.

C. Grid Adjustments

1. Transmission Line Calculation

In this section, we developed a method to calculate the transmission line rating of the 118-busbar system, where the line ratings of this system were not included in the provided MATPOWER case file. This technique is based on surge impedance (SI) and surge impedance loading (SIL). SI is the square-root of the ratio of line inductance to line capacitance, and SIL is defined as the power a transmission line delivers to a load that matches the line's surge impedance.

The case structure introduced resistance, inductive, and capacitive elements, which provided us with a solid foundation for estimating the line parameters. This system has two operating voltages of 138 kV and 345 kV, and as a first step, we extracted the lines and separated them depending on the operating voltages, we calculated the Z_{base}, the SI in per-unit (SI_{pu}), and the SI in ohms (SI_{Ω}) as follows:

$$Z_{base} = \frac{V^2}{S_{base}} \tag{19}$$

$$SI_{pu} = \sqrt{\frac{X_L}{Y_c}} \tag{20}$$

$$SI_{\Omega} = SI_{pu}\ Z_{base} \tag{21}$$

After calculating the SI_{pu} and the SI_{Ω}we are estimated the length of the transmission line, by using an average impedance of $0.39\Omega/\text{km}$ [29]. Using equation (22) to calculate the length of the transmission line base on the line impedance.

$$TL\ length = \frac{X_L\ Z_{base}}{0.39} \tag{22}$$

Referring to Figure 6 we can extract the load ability in per-unit of SIL (SIL_{factor}) for the transmission line based on the transmission line length. The SIL of the transmission line is based on nodal voltage and SI_Ω for each line as follows:

$$SIL = \frac{V_{node}^2}{SI_\Omega} \tag{23}$$

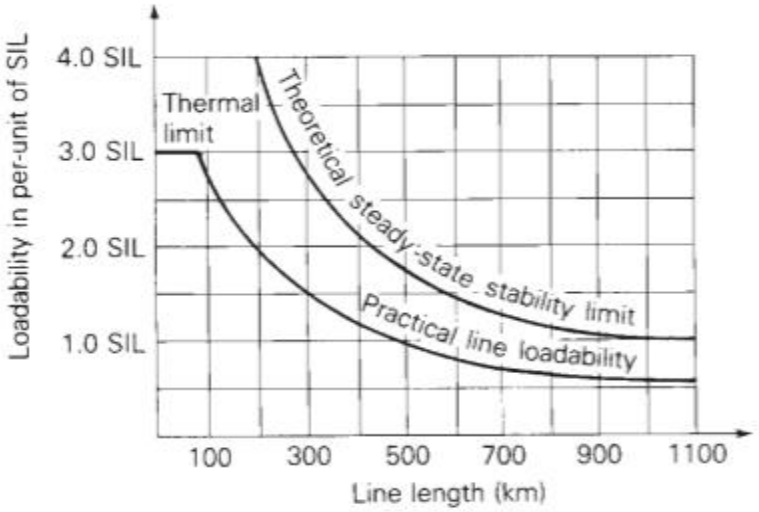

Figure 6: Load-ability in per-unit of SIL

After extracting all line SI and SIL and the length we can calculate the line rating based on the SIL_{factor} and SIL as follows:

$$Line\ Rating = SIL_{factor}\ SIL \tag{24}$$

Before making any adjustments, we analyzed the MATPOWER data to determine whether these branches could be an underground cable, an overhead transmission line, or even a triple or double bundle. We used a book reference to guide our analysis, but this wasn't an accurate estimation.

Two overhead transmission lines and an underground cable were found, despite their connection to the same bus on the other side. To analyze it and determine its type, we calculated the line's diameter as well as its inductance and capacitance.

2. Transformer Calculation

In our model grids, we found that certain transformers do not appear as transformers, but rather as transmission lines in the MATPOWER model, and some transformers have incorrect line estimates. Consequently, we employed a theory to accurately estimate the size of our transformer. This model is used in both the 118-bus and 30-bus systems.

We employ a formula that illustrates both the transformer's reactance and its average leakage to get a reliable estimation of the transformer's size. The average leakage reactance in a HV transformer ranges from 0.08 to 0.12 per-unit, with the 0.12 indicating a conventional quality transformer and the 0.08 indicating a well-equipped ferromagnetic material. In our module, we will use 0.12 since both grids are rather old according to the MATPOWER reference. Given the transformer leakage reactance (X_L) in the "case table", the rating (S_T) in MVA is given by:

$$S_T = \frac{0.12}{X_L} \; S_{base} \tag{25}$$

2. Generator Calculation

In this section, we focused on recalculating the reactive power generation to address inconsistencies identified in the generator data provided by MATPOWER for both the 118-bus and 30-bus systems. Upon analyzing the supplied data, we observed an

illogical ratio between the active and reactive power outputs. A generator demonstrated the ability to deliver 100 MW of active power and 300 MVAr of reactive power concurrently. This proportion between active and reactive power output raises concerns regarding the accuracy of reactive power analysis. Because of this, the reactivity limit had to be recalculated to make sure that the reactive power analysis method for these systems was reliable and valid. Our approach involved adjusting the reactive power capabilities to align with realistic operational constraints, thereby providing a more accurate foundation for subsequent system performance evaluations.

This led to recalculating the reactivity limits of all generators by considering the phase angle 0.95 represented in Eq. 25, relying on the geometric triangle in Figure 7 to extract the maximum reactivity shown in Eq. 26.

$$\cos \varphi = 0.95 \tag{25}$$

$$Q_{max} = P_{max} \tan \varphi \tag{26}$$

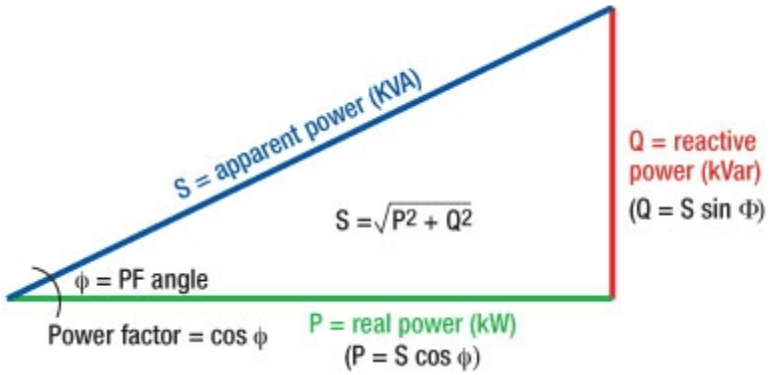

Figure 7: Representation of Power Triangle

D. Calculation

In this section we will display all the economical calculations and battery state of charge calculation we used in our system analysis and formulation.

$$C_{BD} = \frac{I_{BT}\ A_{BT}\ L_{BT}}{DOD_{BT}\ \ N_{BT}\ \ \eta_{\text{inv}}} \tag{27}$$

$$SOC_t = SOC_{t-1} - \frac{1}{\eta_{\text{Dis}}}\frac{P_{t-1}}{E_{BT}} \quad if\ P_{t-1} > 0 \tag{28}$$

$$SOC_t = SOC_{t-1} + \eta_{\text{Cha}}\frac{P_{t-1}}{E_{BT}} \quad if\ P_{t-1} < 0 \tag{29}$$

$$M_{co_2} = HR\ \frac{1}{HV}\ E_G m_{co_2} \tag{30}$$

$$LCOE = \frac{TC_{PV} + TC_{BT} + TC_{DG} + TC_{svc}}{E_T} \tag{31}$$

$$F_c = E_{DG} * \ F_{p/L} \tag{32}$$

$$Capex = \ Investment \times Annuity \times Element\ size \tag{33}$$

$$Opex = Element\ size \times \ Per\ Unit\ Operation\ Cost \tag{34}$$

CHAPTER III

RESULTS

This section presents the results of simulation studies based on our proposed methodologies to assess the performance of the 5-bus classical and renewable micro-grid, Younine 18-bus, IEEE 30 bus, and the 118 bus. In our results a load profile is shown in Figure 8 have been used to run the systems throughout timeline this load profile was derived from a gathered data in 2021. In our results we will demonstrate an economical analysis on our cases such as investment cost, Capex, Opex, fuel cost. These calculations are based on equipment investment and maintenance. Economical values are demonstrated in Table 2 that are extracted from the references [25] and [26].

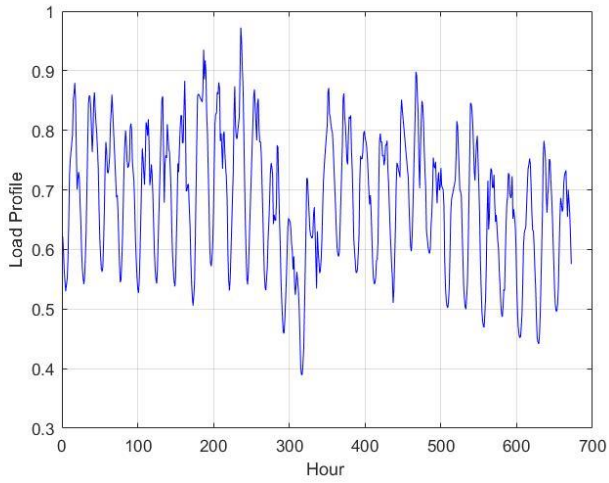

Figure 8: Load Profile

Table 2: Cost Values

PV INV	1.08×10^6 \$/MW	DG FOM	35,000 \$/MW-year
PV OM	16,000 \$/MW-year	DG VOM	5.67 \$/MWh
BT INV	379×10^3 \$/MWh	DG FC	0.88\$/L
BT OM	10,000 \$/MWh-year	DG HR	8295 BTU/kWh
DG INV	330×10^3 \$/MW	SVC INV	80,000 \$/MVAr

A. Case Study: 5-Bus System

1. 5-Bus Classical Grid Study

This section focuses on analyzing a simple adjusted 5-bus classical and renewable microgrid in the 5-bus microgrid, we will apply the transmission line outage methodology for the classical and renewable; however, the reactive support will be applied for the renewable model of microgrid and analyze the outcomes. Figure 9 shows this microgrid, illustrating the interconnections among buses, generators, and transmission lines. Table 3 contains information about each bus in the microgrid, including its type (PV, PQ, RF, isolated), active and reactive loads at each bus, and voltage levels. This table facilitates precise modeling and analysis by identifying each bus's role and attributes. Table 4 is the generator data, which provides a comprehensive overview of the specifications for each generator in the system, including their minimum and maximum capacity, operational constraints, and which bus they are located on. Table 5 displays transmission line data that provides extensive information about each transmission line, including impedance, resistance, rating, connection, and whether the line is in the contingency set. This data is critical for evaluating the lines' capacity to withstand different load conditions and strategizing reinforcements in the event of probable outages.

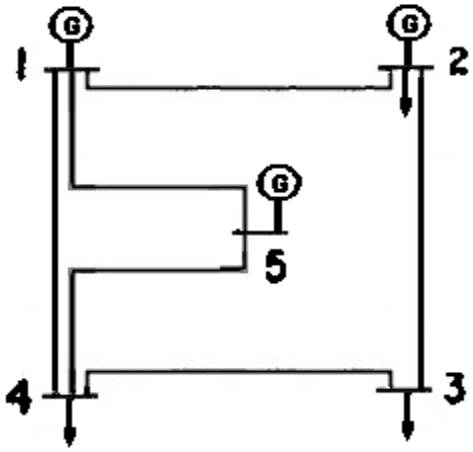

Figure 9: 5-Bus Microgrid

Table 3: 5-Bus Node Data

Node	Type	Active Demand (MW)	Reactive Demand (MVA)	Voltage (KV)
1	PV	0	0	11
2	PQ	2.03	0.67	11
3	PV	2.03	0.67	11
4	RF	2.74	0.89	11
5	PV	0	0	11

Table 4: 5-Bus Generator Data

Node	P_{min} (MW)	P_{max} (MW)	Q_{min} (MVAR)	Q_{max} (MVAR)	Cost ($/MWh)
1	0.6	2.7	0.25	1.16	215
2	0.6	2.7	0.25	1.16	215
5	0.6	2.7	0.25	1.16	215

Table 5: 5-Bus Transmission Data

From	To	Resistance (PU)	Admittance (PU)	Rate (MVA)	Contingency
1	2	0.0316	0.0692	3	Y
1	4	0.0316	0.0692	3	Y
1	5	0.0158	0.0692	3	Y
2	3	0.0158	0.0346	3	Y
3	4	0.0316	0.0692	3	Y
4	5	0.0158	0.0346	3	Y

Using the DC-OPF model, we performed the transmission line outage analysis for the 5-bus system. The results showed that neither the generators nor the transmission lines required any modifications. Our results verify that the 5-bus system functioned effectively during the simulated outage scenarios, sustaining stability and fulfilling demand without necessitating any corrective measures. Table 6 displays the bus data from the DC-OPF, while Table 7 displays the branch flow results.

Table 6: 5-Bus Node Results

Bus	Voltage		Generation		Load	
#	Magnitude	Angle(deg)	P(MW)	Q(MVAr)	P(MW)	Q(MVAr)
1	1	0.363	1.40	-	-	-
2	1	0.055	2.7	-	2.03	-
3	1	-0.232	-	-	2.03	-
4	1	0	-	-	2.74	-
5	1	0.478	2.7	-	-	-

Table 7: 5-Bus Branch Result

From	To	Active From (MW)	Reactive From (MVAR)	Active To (MW)	Reactive To (MVAR)
1	2	0.78	0	-0.78	0
1	4	0.91	0	-0.91	0
1	5	-0.29	0	0.29	0
2	3	-0.58	0	0.58	0
3	4	-0.58	0	0.58	0
4	5	-2.41	0	2.41	0

Next we increase the system demand by 40% and evaluate its capability to supply the increased demand and manage line outages, and determine whether reinforcement is necessary as a future plan for the microgrid. Table 8 lists the peak load adjustments.

Table 8: 5-Bus Data at 40% Demand Increase

Node	Type	Active Demand (MW)	Reactive Demand (MVA)	Base KV
1	PV	0	0	11
2	PQ	2.84	0.94	11
3	PV	2.84	0.94	11
4	REF	3.84	1.24	11
5	PV	0	0	11

Following this 40% increase in demand, the examination of transmission line outages revealed the need for an extra generator. The analysis showed that the incremental costs for all the buses were the same, providing flexibility in selecting the position of the generator. We have reinforced the generator by an additional unit with an active power capacity of 2.7 MW.

The 5-bus microgrid implementation in the line outage showed that the removal of branch (1-4) results in the use of a fictitious generator during line outages. Upon closer inspection, we determined that branch (4-5) had reached its maximum loading capacity and needed reinforcement. After strengthening this branch and then re-executing the line outage using DC-OPF, the system demonstrated robust operation. Table 9 displays the reinforced system's result for the bus data, while Table 10 displays the results for the branch data.

Table 9: 5-Bus Node Results at 40% Demand Increase

Bus	Voltage		Generation		Load	
#	Magnitude	Angle(deg)	P(MW)	Q(MVAr)	P(MW)	Q(MVAr)
1	1	0.62	4.12	-	-	-
2	1	-0.113	2.7	-	2.84	-
3	1	-0.451	-	-	2.84	-
4	1	0	-	-	3.84	-
5	1	0.338	2.7	-	-	-

Table 10: 5-Bus Branch Result at 40% Demand Increase

From	To	Active From (MW)	Reactive From (MVAR)	Active To (MW)	Reactive To (MVAR)
1	2	1.85	0	-1.85	0
1	4	1.56	0	-1.56	0
1	5	0.71	0	-0.71	0
2	3	1.71	0	-1.71	0
3	4	-1.14	0	1.14	0
4	5	-1.71	0	1.71	0
4	5	-1.71	0	1.71	0

2. 5-Bus Micro-Grid with Renewable Energy

This system has the same node and branch data, as well as configuration, of the system of Fig. 9 and was introduced by Salloum [23], where she considered a methodology based on ordinal optimization and DC-OPF for choosing the best allocation and sizing for renewable energy elements PV and BES. We use the methodology described in this research methodology as an optimal for the placement and sizing of photovoltaic (PV) panels and battery energy storage systems (BESS) in our 5-bus system. Table 1 in the previous Chapter, showcased the top 8 designs selected from the best-performing 37 designs. These top designs represent the most efficient configurations based on the criteria established in the methodology.

After simulating these designs of Table 1 and identifying the critical hours for each design, as illustrated earlier, we will simulate the operation of these designs using a the transmission line outage study and analyze the grid's performance.

Running the base case of Design 1 shows that, in the absence of an outage, the grid maintains its integrity and can meet demand and battery charging. However, branch (2-3) is nearing its limit. When we initiate a branch outage and eliminate the first line in the contingency set, it reveals the use of a fictitious generator at node 1, with the branch

(2-3) has reaching its limit and requiring reinforcement. After reinforcing branch (2-3) we restarted our branch outage scenario, and when we removed the branch (1-2) it indicated that a fictitious generator is also being used at node 1. This resulted in an overload in branch (3-4), signaling the need for further reinforcement. After reinforcing the branch. To ensure that our grid performance, we redo again the outage performance, but this time when branch (2-3) is removed, it reflects that a fictitious generator at node 1 has been used and indicates that branch (2-3) must be reinforced again. This also indicated that when we added the first line between node 2 and node 3, it wasn't sufficient, where any failure in these two lines will lead to a loading shedding. Table 11 indicates the nodal voltage with generator supplying demand and battery charging. Table 12 displays the branch flow for all branches after they have been reinforced.

Table 11: 5-Bus Nodal Data with Renewable Energy (Design 1)

Bus	Voltage		Generation		Load	
#	Magnitude	Angle(deg)	P(MW)	Q(MVAr)	P(MW)	Q(MVAr)
1	1	0.83	5.7	-	-	-
2	1	-0.038	3.24	-	1.47	-
3	1	-0.3	2.23	-	7.71	-
4	1	0	0	-	1.99	-
5	1	0.278	0	-	-	-

Table 12: 5-Bus Transmission Line Flow with Renewable Energy (Design 1)

From	To	Active From (MW)	Reactive From (MVAR)	Active To (MW)	Reactive To (MVAR)
1	2	2.20	0	-2.20	0
1	4	2.10	0	-2.10	0
1	5	1.40	0	-1.40	0
2	3	1.32	0	-1.32	0
3	4	-0.76	0	0.76	0
4	5	-1.40	0	1.40	0
2	3	1.32	0	-1.32	0
3	4	-0.76	0	0.76	0
2	3	1.32	0	-1.32	0

Similarly, after running Design 2 it also indicates that we must reinforce the same lines leading to the same results as Design 1. However, when executing design 3 and 7 in the base case, it appears that line (2-3) has reached its limit. This is evident in the initial branch outage on line (1-2), suggesting the use of a fictitious generator at node 1. Once we reinforce line (2-3) and restart the line outage, there is a use of fictitious generator at node 1 when we remove branch (1-2). In this case, branch (3-4) has reached its limit, indicating the need for reinforcement. After carrying out these reinforcements our grid seems secure and dependable. The node results of the reinforced micro-grid are shown in Table 13, the branch flows of the reinforced micro-grid are shown in Table 14.

Table 13: 5-Bus Nodal Data with Renewable Energy (Design 3)

Bus	Voltage		Generation		Load	
#	Magnitude	Angle (deg)	P(MW)	Q(MVAr)	P(MW)	Q(MVAr)
1	1	0.83	5.58	-	-	-
2	1	0.058	3.24	-	1.47	-
3	1	-0.316	2.35	-	7.71	-
4	1	0	0	-	1.99	-
5	1	0	0	-	-	-

Table 14: 5-Bus Transmission Line Flow with Renewable Energy (Design 3)

From	To	Active From (MW)	Reactive From (MVAR)	Active To (MW)	Reactive To (MVAR)
1	2	2.0	0	-2.0	0
1	4	2.15	0	-2.15	0
1	5	1.43	0	-1.43	0
2	3	1.89	0	-1.89	0
3	4	-0.80	0	0.80	0
4	5	-1.43	0	1.43	0
2	3	1.89	0	-1.89	0
3	4	-0.80	0	0.80	0

Executing design 4,5, 6, and 8 in the transmission line outage indicates a weakness in lines (2-3), (3-4), and (1-4). In this design, a new line reinforcement has been indicated. Reflecting that sizing elements is a crucial element that affects transmission lines.

Table 15: 5-Bus Nodal Data with Renewable Energy (Design 4)

Bus	Voltage		Generation		Load	
#	Magnitude	Angle(deg)	P(MW)	Q(MVAr)	P(MW)	Q(MVAr)
1	1	0.613	5.85	-	-	-
2	1	-0.07	3.31	-	1.47	-
3	1	-0.424	2.76	-	8.46	-
4	1	0	0	-	1.99	-
5	1	0	0	-	-	-

Table 16: 5-Bus Transmission Line Flow with Renewable Energy (Design 4)

From	To	Active From (MW)	Reactive From (MVAR)	Active To (MW)	Reactive To (MVAR)
1	2	1.72	0	-1.72	0
1	4	1.55	0	-1.55	0
1	5	1.03	0	-1.03	0
2	3	1.78	0	-1.78	0
3	4	-1.07	0	1.07	0
4	5	-1.03	0	1.03	0
2	3	1.78	0	-1.78	0
3	4	-1.07	0	-1.07	0
1	4	1.55	0	1.55	0

Running designs 1, 2, 3, 4, 5, 6, 7, and 8 using the transmission line outage indicates that the grid requires a transmission reinforcement in order to make it adequate. Removing each branch from the 5-bus renewable micro-grid system and running it at 10:00 am, which is the critical hour, indicates that the solar panels are capable of supplying the load and producing excess power to charge the batteries, but at this time transmission lines are observed to be at their highest loading, and as such the different proposed designs are adequate according to the “N – 1” rule.

After the branch reinforcement study, we test the reactive power requirements of each design during our timeline. Here, we will examine the designs at each hour of the load timeline profile using the AC-OPF, and determine whether the available reactive power sources are sufficient or whether we need to add SVC at system nodes. The results these simulations of our microgrid are shown in Table 17, which offer us a valuable insight into the cost-effectiveness and performance of the 8 designs. We note that Designs 3 and 7 require SVC reinforcement at node 5. We also note that the addition of an SVC at node 5 is not necessary as the system is able to supply the reactive demand, however, the use of the SVC reduced transmission losses and thus lowered the LCOE of the system. The best design obtained, from the economic viewpoint, is Design 1 with the lowest LCOE at \$0.2178/ kWh. However, this comes at the disadvantage of using more diesel in the generators with 54.698 tons of CO_2 in Design 1 as compared to 49.249 tons of CO_2 in Design 3. Let us also note that the transmission reinforcements in Designs 1 and 2 are the same, however, the slight increase of battery capacity made Design 2 consume less DG fuel that led to lower CO_2 emissions. Let us also note that the total investment includes the cost of PV, BT, transmission reinforcements, and the needed SVC. Figure 10 shows the energy supply from different sources at different hours within the timeline.

Table 17: 5-Bus Results AC-OPF

Design	PV Size MW	BT Size MWh	DG Size MW	SVC Size MVAR	Total Invest. M$	Total Capex M$/year	Total Opex M$/year	DG Fuel Cost M$/year	Total Energy MWh	LCOE $/kWh	CO_2 tons/ year
1	30	64	8.1	0	57.40	6.29	1.47	1.139	40863	0.2178	54698
2	30	66	8.1	0	58.16	6.40	1.49	1.098	40861	0.2199	52690
3	30	68	8.1	0.286	58.75	6.49	1.51	1.023	40867	0.2209	49249
5	32	64	8.1	0	59.75	6.49	1.51	1.062	40854	0.2216	50983
4	32	62	8.1	0	58.99	6.38	1.49	1.206	40848	0.2221	57866
7	30	70	8.1	0.278	59.51	6.60	1.53	1.045	40863	0.2245	50161
6	32	66	8.1	0	60.50	6.59	1.53	1.072	40854	0.2250	51439
8	32	68	8.1	0	61.26	6.70	1.54	0.965	40856	0.2254	46342

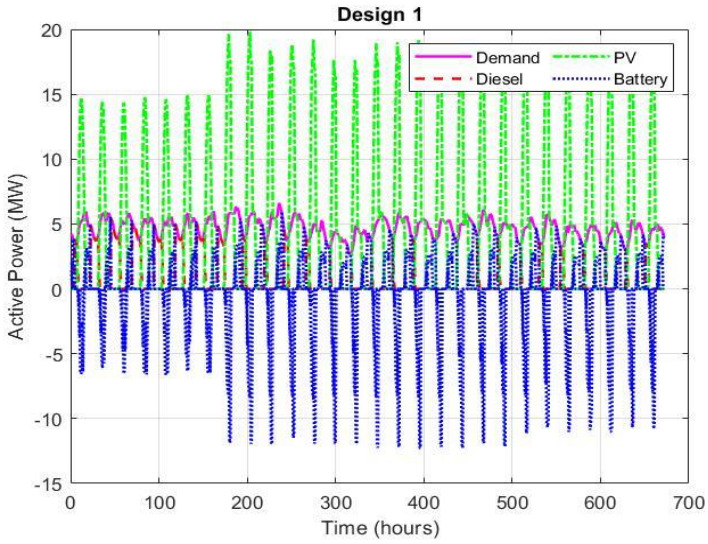

Figure 10: 5-Bus Design 1 active flow versus time

B. Case Study: Younine 18-Bus System

The 18-bus system is a radial system where it is not possible to implement the transmission line outage study, however, here we will apply the AC-OPF study to insure that the system is able to manage the power flows and determine if the system require any additional reactive resources.

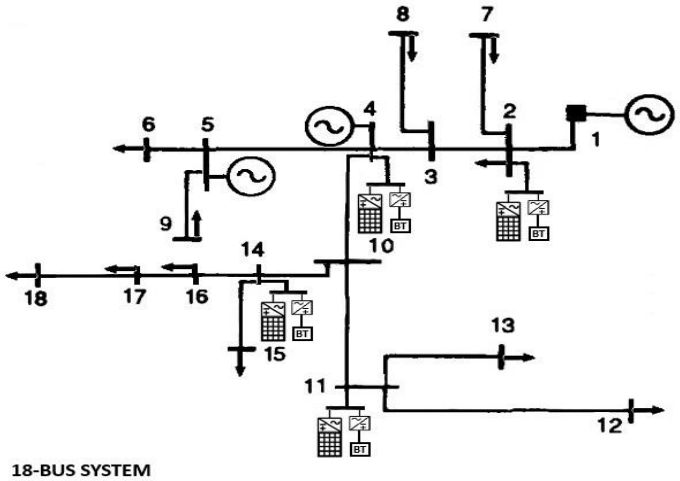

Figure 11: The Younine 18-Bus System

The 18-bus system consists of 18 buses, 3 generators, 11 loaded nodes, and 4 nodes that have renewable energy elements PV and BESS. Displaying the bus, generator and branch data before applying the AC-OPF for the multiple designs. Table 18, 19 and 20 provide information of the bus data, generator data and branch data, respectively.

Table 18: 18-Bus Node Data

Node	Type	Active Demand (MW)	Reactive Demand (MVA)	Base KV
1	PV	0	0	15
2	PQ	0.34	0.112	15
3	PV	0	0	15
4	PV	0	0	15
5	PV	0	0	15
6	PQ	1.36	0.446	15
7	PQ	0.34	0.112	15
8	PQ	1.02	0.335	15
9	PQ	0.68	0.223	15
10	PV	0	0	15
11	PV	0	0	15
12	PQ	1.36	0.446	15
13	PQ	0.34	0.112	15
14	PV	0	0	15
15	PQ	0.34	0.112	15
16	PQ	0.34	0.112	15
17	PQ	0.34	0.112	15
18	RF	0.34	0.112	15

Table 19: 18-Bus Generator Data

Node	P_{min} (MW)	P_{max} (MW)	Q_{min} (MVAR)	Q_{max} (MVAR)	Cost ($/MWh)
1	0.6	2.7	0.25	1.16	215
4	0.6	2.7	0.25	1.16	215
5	0.6	2.7	0.25	1.16	215

Table 20: 18-Bus Transmission Data

From	To	Resistance (PU)	Admittance (PU)	Rating (MVA)
1	2	0.026	0.035	11
2	3	0.026	0.035	11
2	7	0.056	0.030	5
3	4	0.018	0.024	11
3	8	0.050	0.027	5
4	5	0.050	0.027	5
4	10	0.005	0.003	9
5	6	0.040	0.023	5
5	9	0.020	0.023	5
10	11	0.020	0.011	5
10	14	0.030	0.017	5
11	12	0.030	0.017	5
11	13	0.010	0.007	9
14	15	0.050	0.029	5
14	16	0.010	0.054	5
16	17	0.060	0.032	5
17	18	0.026	0.014	5

Designs having different sizes of the PV panels and batteries, at selected nodes, were developed in a study by Salloum [24], and are shown in Table 21. These designs are ranked from the lowest to the highest LCOE (not shown) using the DC-OPF. We will now apply to these designs the AC-OPF aiming to re-evaluate their cost-effectiveness, while verifying whether they require reactive reinforcement or not. Each design has been simulated over the period of representative weeks, encompassing the four seasons. Table 22 shows the results of these studies that reflect a change in the ranking of the different designs, where design 5 now appear to have the lowest LCOE at \$0.2155/ kWh with a midrange amount of CO_2 emissions at 50.931 tons per year. Design 20, on the other hand, has a higher battery size that led to a lower DG fuel consumption leading to a higher LCOE at \$0.222/ kWh but lower emissions at 46.772 tons of CO2 per year. Table 23 indicates the SVC node placement and sizes for the designs that required it.

Table 21: Top 20 Designs of the Younine 18-Bus System

Design	PV Size MW	Battery Capacity MWh	PV Nodes				Battery Nodes			
			2	4	11	14	2	4	11	14
1	30	64	3	16	5	6	35	3	26	0
2	30	66	3	16	5	6	40	3	23	0
3	30	68	4	15	5	6	45	3	20	0
4	32	64	2	18	7	5	30	3	31	0
5	32	62	3	17	6	6	28	4	30	0
6	32	66	3	18	6	5	36	3	27	0
7	30	70	3	14	6	7	50	3	17	0
8	32	70	3	17	5	7	46	3	21	0
9	34	64	4	17	5	8	38	2	24	0
10	34	66	3	17	7	7	46	2	18	0
11	30	72	4	14	4	8	56	5	11	0
12	32	72	3	17	6	6	41	2	29	0
13	34	68	3	18	8	5	37	4	27	0
14	34	70	3	18	7	6	42	4	24	0
15	34	72	3	18	7	6	47	4	21	0
16	36	66	4	19	7	6	40	4	22	0
17	36	68	4	18	7	7	48	3	17	0
18	34	74	3	18	7	6	50	3	20	1
19	36	70	4	19	6	7	46	4	20	0
20	32	68	3	18	6	5	41	3	24	0

Table 22: Younine 18-Bus Results AC-OPF

Design	**PV Size MW**	**BT Size MWh**	**DG Size MW**	**SVC Size MVAR**	**Total Invest. M$**	**Total Capex M$/year**	**Total Opex M$/year**	**DG Fuel Cost M$/year**	**Total Energy MWh**	**LCOE $/ kWh**	**CO_2 tons/ year**
5	32	62	8.1	0.349	58.09	6.31	1.50	1.061	41197	0.21554	50931
1	30	64	8.1	0	56.66	6.23	1.50	1.252	41190	0.21809	60095
2	30	66	8.1	0	57.43	6.34	1.52	1.172	41264	0.21888	56262
3	30	68	8.1	0	58.17	6.45	1.53	1.084	41330	0.21938	52039
7	30	70	8.1	0	58.93	6.56	1.55	0.993	41396	0.21987	47685
4	32	64	8.1	0.281	58.84	6.42	1.53	1.146	41229	0.22057	54998
9	34	64	8.1	0	60.98	6.60	1.55	0.992	41286	0.22167	47646
20	32	68	8.1	0	60.33	6.63	1.56	0.974	41362	0.22174	46772
10	34	66	8.1	0	61.73	6.71	1.57	0.938	41416	0.22272	45038
6	32	66	8.1	0.296	59.60	6.53	1.55	1.157	41269	0.22374	55532
8	32	70	8.1	0	61.09	6.74	1.58	0.93	41348	0.22381	44660
11	30	72	8.1	0.474	59.73	6.67	1.57	1.05	41351	0.22472	50435
16	36	66	8.1	0	63.89	6.90	1.60	0.834	41372	0.22562	40033
13	34	68	8.1	0.33	62.52	6.82	1.59	0.915	41327	0.22579	43930
14	34	70	8.1	0	63.25	6.93	1.61	0.85	41374	0.22694	40815
15	34	72	8.1	0	64.01	7.04	1.63	0.792	41426	0.22831	38025
17	36	68	8.1	0	64.65	7.01	1.62	0.851	41471	0.22859	40841
12	32	72	8.1	0	61.86	6.85	1.60	0.995	41287	0.22888	47776
19	36	70	8.1	0	65.02	7.08	1.64	0.815	41429	0.23008	39146
18	34	74	8.1	0.426	64.80	7.15	1.65	0.78	41421	0.23122	37465

Table 23: SVC Placement and Sizes (MVAr) for Younine 18-Bus System

Nodes/ Designs	5	4	6	11	13	18
1	0.021	0.018	0.019	0.016	0.021	0.015
2	0.02	0.016	0.017	0.009	0.019	0.007
3	0.019	0.014	0.015	0.02	0.017	0.018
4	0.018	0.012	0.013	0.025	0.014	0.022
5	0.02	0.017	0.018	0.031	0.02	0.029
6	0.018	0.013	0.014	0.031	0.015	0.029
7	0.02	0.015	0.016	0.016	0.018	0.015
8	0.018	0.013	0.013	0.024	0.015	0.022
9	0.02	0.015	0.016	0.031	0.017	0.029
10	0.019	0.015	0.015	0.028	0.017	0.025
11	0.019	0.015	0.016	0.025	0.017	0.019
12	0.017	0.014	0.015	0.028	0.016	0.023
13	0.019	0.016	0.017	0.027	0.018	0.022
14	0.02	0.017	0.018	0.032	0.02	0.03
15	0.02	0.018	0.019	0.032	0.021	0.03
16	0.02	0.018	0.019	0.033	0.021	0.03
17	0.02	0.018	0.019	0.033	0.022	0.03
18	0.02	0.018	0.019	0.033	0.022	0.03

C. Case Study: IEEE 30-Bus System

This section focuses on analyzing the IEEE 30-bus system to illustrate the application of our methodology to assess the transmission adequacy of a relatively larger system size. The system consists of 30 nodes, 43 branches, and five generators capable of supplying 295 MW and 103 MVAr, with a total peak demand of 189 MW and 107 MVAr.

Let us first note that the data provided in the MATPOWER (MP) file are not compatible when compared to the available diagram [27], shown in Figure 12. We found that some branches are missing and that reactive limits are not the usual norm of reactive generation capability. One branch between buses 1 and 2 along with a branch between buses 10 and 21 were missing. The MP data indicated that all buses operate at 135 kV, which did not reflect the presence of transformers. However, after visiting other sources

of data we found out that this system operates at three voltage levels: 11, 33, and 132 KV. Tables 24, 25, and 26 contain comprehensive specifications for the buses, generators, and branches, respectively after the modifications we have carried out. The tables offer a detailed perspective of every aspect of the system, such as voltage levels, generation capacity, and transmission line specifications. This enables a comprehensive examination of the 30-bus grid. By utilizing this improved and precisely designed 30-bus grid, we can conduct comprehensive simulations to assess the system's efficiency, detect potential weaknesses, and implement necessary enhancements to ensure a stable and dependable operation.

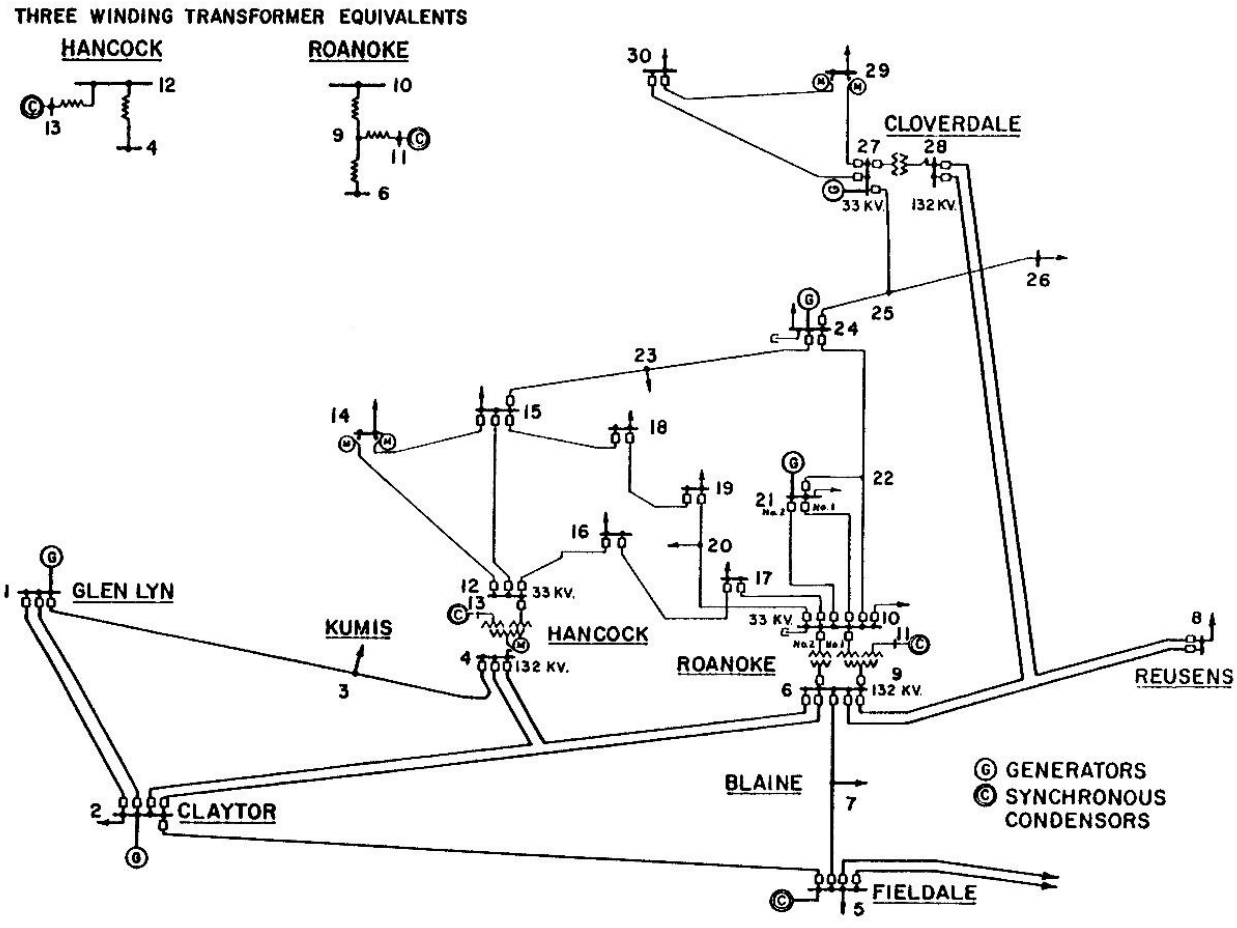

Figure 12: IEEE 30-Bus Grid

Table 24: IEEE 30-Bus Node Data

Node	Type	Active Demand (MW)	Reactive Demand (MVA)	Base kV
1	RF	0	0	132
2	PV	21.7	12.7	132
3	PQ	2.4	1.2	132
4	PQ	7.6	1.6	132
5	PQ	0	0	132
6	PQ	0	0	132
7	PQ	22.8	10.9	132
8	PQ	30	30	132
9	PQ	0	0	11
10	PQ	5.8	2	33
11	PQ	0	0	33
12	PQ	11.2	0	33
13	PV	0	0	11
14	PQ	6.2	1.6	33
15	PQ	8.2	2.5	33
16	PQ	3.5	1.8	33
17	PQ	9	5.8	33
18	PQ	3.2	0.9	33
19	PQ	9.5	3.4	33
20	PQ	2.2	0.7	33
21	PQ	17.5	11.2	33
22	PV	0	0	33
23	PV	3.2	1.6	33
24	PQ	8.7	6.7	33
25	PQ	0	0	33
26	PQ	3.5	2.3	33
27	PV	0	0	33
28	PQ	0	0	132
29	PQ	2.4	0.9	33
30	PQ	10.6	1.9	33

Table 25: IEEE 30-Bus Generator Data

Node	$P_{\min}$ (MW)	$P_{\max}$ (MW)	$Q_{\min}$ (MVAR)	$Q_{\max}$ (MVAR)	Cost ($/MWh)
1	24	80	-13	26	215
2	24	80	-13	26	215
21	17	50	-8	15	215
24	9	30	-5	19	215
27	17	55	-9	17	215

Table 26: IEEE 30-Bus Transmission Data

From	To	Resistance (PU)	Admittance (PU)	Rate (MVA)	Contingency
1	2	0.0384	0.1150	130	N
1	2	0.0384	0.1150	130	Y
1	3	0.0452	0.1652	130	Y
2	4	0.0570	0.1737	100	Y
3	4	0.0132	0.0379	130	Y
2	5	0.0472	0.1983	130	Y
2	6	0.0581	0.1763	100	Y
4	6	0.0119	0.0414	100	Y
5	7	0.0460	0.1160	100	Y
6	7	0.0267	0.0820	130	Y
6	8	0.0120	0.0420	130	Y
6	9	0.00	0.2080	65	N
6	10	0.00	0.5560	32	N
9	11	0.00	0.2080	65	N
9	10	0.00	0.1100	65	N
4	12	0.00	0.2560	65	N
12	13	0.00	0.1400	65	N
12	14	0.1231	0.2559	32	Y
12	15	0.0662	0.1304	32	Y
12	16	0.0945	0.1987	32	Y
14	15	0.2210	0.1997	16	Y
16	17	0.0524	0.1923	16	Y
15	18	0.1073	0.2185	16	Y
18	19	0.0639	0.1292	16	Y
19	20	0.0340	0.0680	32	Y
10	20	0.0936	0.2090	32	Y
10	17	0.0324	0.0845	32	Y
10	21	0.0696	0.1498	32	N
10	21	0.0696	0.1498	32	Y
10	22	0.0727	0.1499	32	Y
21	22	0.0116	0.0236	32	Y
15	23	0.1000	0.2020	16	Y
22	24	0.1150	0.1790	16	Y
23	24	0.1320	0.2700	16	Y
24	25	0.1885	0.3292	16	Y
25	26	0.2544	0.3800	16	N
25	27	0.1093	0.2087	16	Y
28	27	0.00	0.3960	65	N
27	29	0.2198	0.4153	16	Y
27	30	0.3202	0.6027	16	Y
29	30	0.2399	0.4533	16	Y
8	28	0.0636	0.2000	130	Y
6	28	0.0169	0.0599	130	Y

After addressing the adjustments on the 30-bus system, we applied the transmission line outage study at peak demand conditions to evaluate the system's transmission and generation capabilities and determine if any reinforcement is necessary. During the outage study, we considered that the units on bus 1 and 2 consist of 2 units, where each can supply 40 MW, and we turned off one unit at each node to reflect the usual practice during system operation of having one unit on outage and one on maintenance. The outage study revealed that neither the generators nor the transmission lines needed any reinforcement. The assessment of this system using the AC-OPF tool revealed that we need to add SVC with an overall size of 4.04 MVAR as shown in Table 27, the SVC's are distributed on 4 nodes as shown in Table 28. The total generation profile during the selected time is shown in Fig. 13.

Table 27: IEEE 30-Bus Summary Table

Generator size (MW)	**SVC size (MVAR)**	**Total Investment (M$)**	**Total Capex (M$/year)**	**Total Opex (M$/year)**	**Fuel Cost (M$/year)**	**Total Energy Produced (MWh)**	**LCOE ($/kWh)**	**CO_2 tons/ year**
215	4.04	0.32	0.04	26.88	245.7	1142770	0.2385	11,796

Table 28: IEEE 30-Bus SVC Placement and Sizes

Nodes	SVC Size (MVAR)
14	0.98
16	0.23
18	0.41
19	2.42

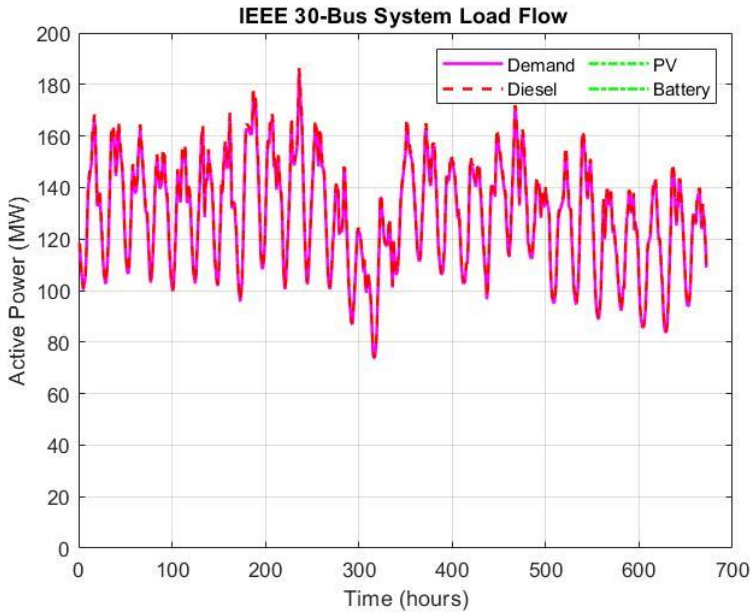

Figure 13: IEEE 30-Bus Load Flow versus Time

Then we increased the demand by 50% and repeated the outage study. However, we noted that the capacity of the generators is now less than the system peak demand; the generators have a power of 215 MW while the demand with 50% increase is now at 284 MW. Therefore, to address this situation, we added reinforcement generators at candidate nodes, which will be turned ON when needed. During the base case DC-OPF, fictitious generators are used at node 3, which led to turning on reinforcement generator located at node 1, with active power 40 MW, due to equal incremental cost at all nodes. However, this was not sufficient, and a further usage of a fictitious generator is noted at node 15 that led to the turning on another reinforcement generator located at node 2 with active power capacity of 40 MW. A further addition of a reinforcement generator of capacity 50 MW was added at node 15 that had the highest incremental cost among generator reinforcements.

After reinforcing the generator system, we start the line outage study using the DC-OPF tool. The removal of branch (19–20) caused the activation of a fictitious generator at node 19, which led to branch (15-18) to operate at its maximum limit, indicating the need for reinforcement. We reinforced this branch by adding a similar one in parallel to increase its power carrying capability. Further contingencies showed that also branch (27-30) needs to be reinforced. After reinforcing the mentioned branches system appears to be adequate with the base case results as shown in Tables 28 and 29.

Table 29: IEEE 30-Bus Node Results (50% Demand Increase)

Bus	Voltage		Generation		Load	
#	Magnitude	Angle(deg)	P(MW)	Q(MVAr)	P(MW)	Q(MVAr)
1	1	0.00	80.00	-	-	-
2	1	-1.15	48.00	-	32.55	-
3	1	-2.98	-	-	3.60	-
4	1	-3.88	-	-	11.40	-
5	1	-3.61	-	-	-	-
6	1	-4.57	-	-	-	-
7	1	-5.05	-	-	34.20	-
8	1	-5.39	-	-	45.00	-
9	1	-6.06	-	-	-	-
10	1	-6.85	-	-	8.70	-
11	1	-6.06	-	-	-	-
12	1	-8.47	-	-	16.80	-
13	1	-8.47	-	-	-	-
14	1	-9.44	-	-	9.30	-
15	1	-9.20	50.00	-	12.30	-
16	1	-8.37	-	-	5.25	-
17	1	-7.74	-	-	13.50	-
18	1	-9.45	-	-	4.80	-
19	1	-9.41	-	-	14.25	-
20	1	-8.87	-	-	3.30	-
21	1	-6.13	50.00	-	26.25	-
22	1	-6.25	-	-	-	-
23	1	-8.31	-	-	4.80	-
24	1	-6.43	9.00	-	13.05	-
25	1	-4.34	-	-	-	-
26	1	-5.40	-	-	5.25	-
27	1	-2.42	46.80	-	-	-
28	1	-4.52	-	-	-	-
29	1	-4.44	-	-	3.60	-
30	1	-5.78	-	-	15.90	-

Table 30: IEEE 30-Bus Transmission Line Results (50% Demand Increase)

From	To	Active From (MW)	Reactive From (MVAR)	Active To (MW)	Reactive To (MVAR)
1	2	21.74	0.00	-21.74	0.00
1	2	21.74	0.00	-21.74	0.00
1	3	36.51	0.00	-36.51	0.00
2	4	17.83	0.00	-17.83	0.00
3	4	32.91	0.00	-32.91	0.00
2	5	17.55	0.00	-17.55	0.00
2	6	23.55	0.00	-23.55	0.00
4	6	29.12	0.00	-29.12	0.00
5	7	17.55	0.00	-17.55	0.00
6	7	16.65	0.00	-16.65	0.00
6	8	35.97	0.00	-35.97	0.00
6	9	3.19	0.00	-3.19	0.00
6	10	1.82	0.00	-1.82	0.00
9	11	0.00	0.00	0.00	0.00
9	10	3.19	0.00	-3.19	0.00
4	12	10.22	0.00	-10.22	0.00
12	13	0.00	0.00	0.00	0.00
12	14	0.68	0.00	-0.68	0.00
12	15	-11.87	0.00	11.87	0.00
12	16	4.62	0.00	-4.62	0.00
14	15	-8.62	0.00	8.62	0.00
16	17	-0.63	0.00	0.63	0.00
15	18	7.51	0.00	-7.51	0.00
18	19	10.21	0.00	-10.21	0.00
19	20	-4.04	0.00	4.04	0.00
10	20	7.34	0.00	-7.34	0.00
10	17	14.13	0.00	-14.13	0.00
10	21	-8.72	0.00	8.72	0.00
10	21	-8.72	0.00	8.72	0.00
10	22	-7.72	0.00	7.72	0.00
21	22	6.31	0.00	-6.31	0.00
15	23	2.19	0.00	-2.19	0.00
22	24	-1.41	0.00	1.41	0.00
23	24	-2.61	0.00	2.61	0.00
24	25	-8.07	0.00	8.07	0.00
25	26	5.25	0.00	-5.25	0.00
25	27	-13.32	0.00	13.32	0.00
28	27	-13.98	0.00	13.98	0.00
27	29	6.42	0.00	-6.42	0.00
27	30	6.54	0.00	-6.54	0.00
29	30	2.82	0.00	-2.82	0.00
8	28	-9.03	0.00	9.03	0.00
6	28	-4.95	0.00	4.95	0.00
15	18	7.51	0.00	-7.51	0.00
27	30	6.54	0.00	-6.54	0.00

After confirming that the 30-bus grid is well-reinforced at normal system operation from the transmission line and generator perspective, we proceed to analyze our system using the AC-OPF tool, to determine whether the grid needs reactive support, in addition to that available on generators. When we carried out the AC-OPF on the system, the results revealed that the available reactive resources are capable of handling the reactive demand without the use of SVC as shown in Table 2. The total generation profile during the selected time is shown in Fig. 14.

Table 31: 30-Bus Summary Table with SVC (50% Demand Increase)

Gen. size MW	**SVC size MVAR**	**Total Investment M$**	**Total Capex M$/year**	**Total Opex M$/year**	**Fuel Cost M$/year**	**Total Energy Produced MWh**	**LCOE $/kWh**	**CO_2 ton/ year**
345	0	388.8	29.78	39.8	368	1,711,188	0.2556	17,664

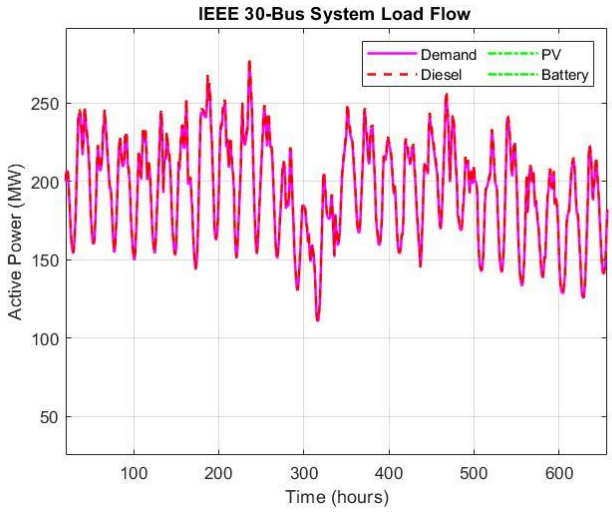

Figure 14: IEEE 30-Bus demand profile versus time at 50% demand increase.

D. Case Study: IEEE 118-Bus System

The IEEE 118-bus system, presented in Figure 15, is a relatively large power grid to further illustrate the ability of our planning tool to handle such large systems. Our planning tool entails applying a transmission line outage methodology to this system to assess its performance in the event of a line loss. Then to apply the AC-OPF methodology on the grid in order to evaluate if the system requires any reactive reinforcement.

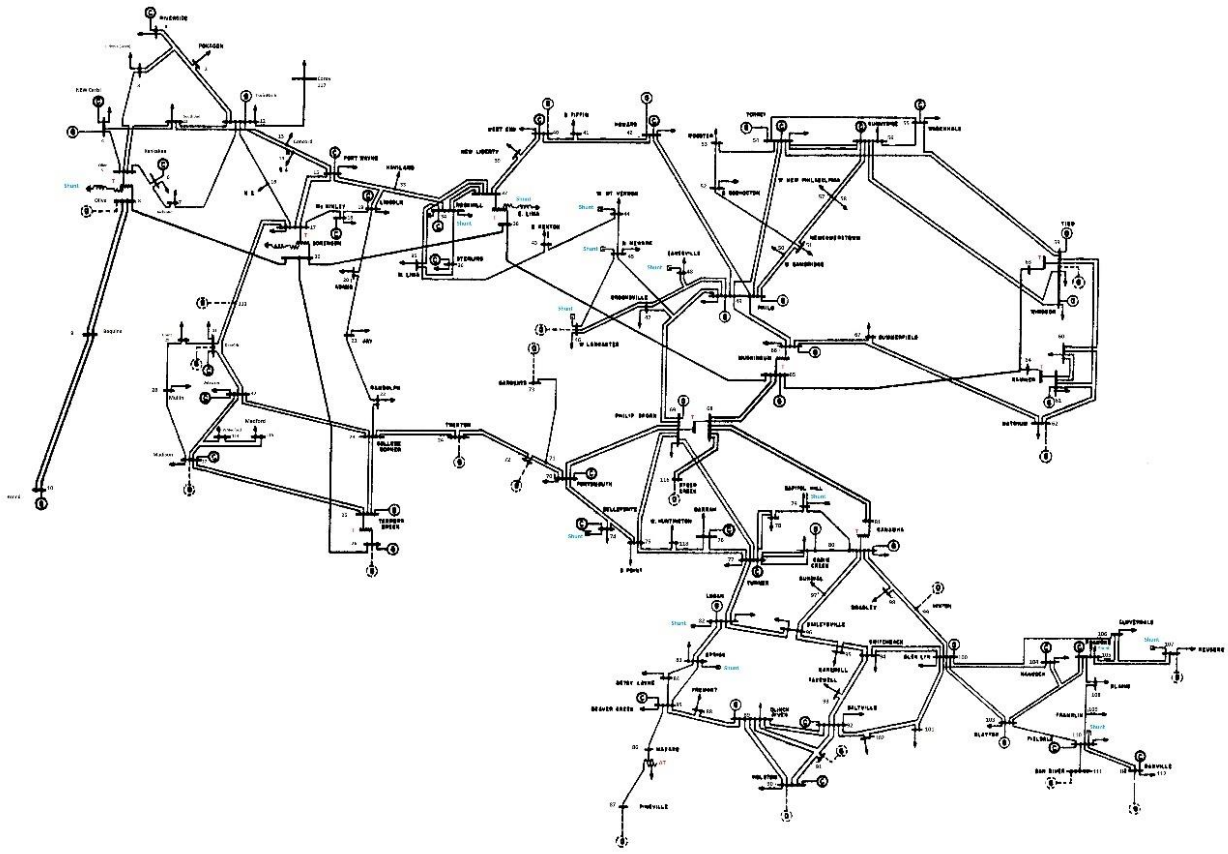

Figure 15: IEEE 118-Bus System

When analyzing the data from the MATPOWER case, we noted that the MVA ratings for all branches in the system were missing. In addition, we noted inaccuracies in the transmission line parameters, which led us to a comprehensive re-evaluation of all branch data. Using our transmission line calculation methodology, on Page 40, we

corrected line parameters and line ratings. The 118-bus system connection diagram was obtained from the literature [28] and is shown in Figure 11. Some lines were missing in the MATPOWER case data, which were added to the MATPOWER data case: these lines were 8-9, 9-10, 15-17, 23-24, 23-25, 25-27, 23-32, 34-37, 54-56, 60-61, 65-68, 69-70, 69-75, 69-77, 77-78, 77-80, 68-81, 77-82, 82-83, 82-96, 94-100, 100-103, 110-112, 68-116. Moreover, we adjusted the transmission line parameters of the following lines: 56-59, 83-84, 84-85, 85-86, 89-90, 89-92, and 92-100. The transformer ratings were also missing, which prompted us to determine them using the transformer rating calculation methodology, outlined on Page 44. In addition, some generator reactive limits were completely off and required adjustments: for example the generator at Node 8 had a power rating of 100 MW and a reactive power capability of 300 MVAr. We adjusted the reactive capability base on a rated power of 0.95.

Before applying the line outage methodology, to the IEEE 118-bus, we also put two units, one on outage and one unit is on maintenance. Then we applied the line outage methodology on this system with the demand being at the current level as shown in the Appendix A1.0. The IEEE 118-bus is comprised of 54 generators, 54 load nodes, 210 branches, and 12 transformers. The generators supply capability are 9966 MW and 3284 MVAr, and the demand is 4242 MW and 1438 MVAr. Two voltages were involved in this system 138 kV and 345 kV.

Applying the transmission line outage study on the 118-bus system revealed that neither the generators nor the transmission lines needed any modifications. The results validate that the 118-bus system is adequate and able to sustain the peak demand during the simulated outage scenarios. Next, we assess whether the 118-bus system requires any

reactive support by applying the AC-OPF on it during four representative weeks. The results show that the IEEE 118 bus system needs reactive power reinforcement from SVC as shown in Table 32. These were placed at several nodes as shown in Table 33. Figure 16 shows the total active power generated by the system versus time.

Table 32: 118-Bus Summary Table with SVC (Base Demand)

Gen. size MW	**SVC size MVAR**	**Total Investment M$**	**Total Capex M$/year**	**Total Opex M$/year**	**Fuel Cost M$/year**	**Total Energy Produced MWh**	**LCOE $/kWh**	**CO_2 ton/ year**
9068	935	74.8	8.2	677.4	5461	25,402,358	0.2419	262,206
8198	0.0	0.0	0.0	647.1	5470	25,441,660	0.2404	262,618

Table 33: IEEE 118-Bus SVC Placements and Sizes

Node	SVC Size	Node	SVC Size	Node	SVC Size
1	6.336	41	8.197	81	15.988
2	6.72	42	8.706	82	10.187
3	5.845	43	5.69	83	9.979
4	4.256	44	5.679	84	10.617
5	4.276	45	6.568	85	12.508
6	4.67	46	6.894	86	10.863
7	5.721	47	8.323	87	10.045
8	2.876	48	7.539	88	14.212
9	2.48	49	9.389	89	18.048
10	1.855	50	9.03	90	20.3
11	5.299	51	9.496	91	16.911
12	6.017	52	9.411	92	14.42
13	5.756	53	11.087	93	12.361
14	6.035	54	13.379	94	12.517
15	5.457	55	14.396	95	13.273
16	5.949	56	12.979	96	11.176
17	5.253	57	9.863	97	10.844
18	5.417	58	10.104	98	11.121
19	5.576	59	16.573	99	11.438
20	6.441	60	13.711	100	12.703
21	6.714	61	14.638	101	11.913
22	6.872	62	13.059	102	12.223
23	6.901	63	21.983	103	12.211
24	7.348	64	20.003	104	11.943
25	6.097	65	18.4008	105	10.456
26	4.733	66	9.12	106	10.524
27	7.216	67	10.785	107	10.097
28	7.47	68	19.239	108	9.784
29	7.296	69	11.157	109	10.156
30	4.619	70	11.404	110	11.726
31	6.992	71	11.403	111	12.032
32	6.991	72	9.297	112	12.312
33	5.728	73	11.487	113	5.497
34	5.993	74	12.568	114	7.36
35	6.214	75	12.064	115	7.466
36	6.102	76	15.251	116	21.279
37	5.345	77	12.002	117	6.937
38	1.909	78	12.095	118	13.634
39	6.952	79	11.348		
40	7.601	80	11.379		

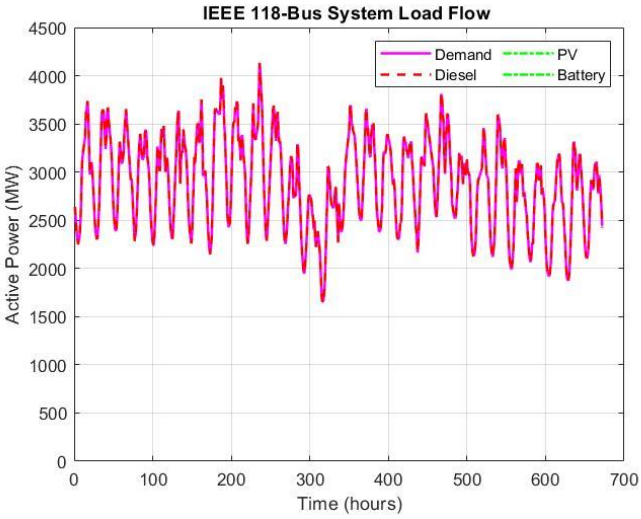

Figure 16: IEEE 118-Bus active demand versus time

Then we increased the demand by 50% and repeated the outage study. During the outage study, we considered that the units on bus 69 and 89 consist of 2 units, where the unit at node 69 can supply 400 out of the available 800 MW, and the at node 89 can supply 350 out of 700 MW available. This is done to reflect the usual practice during system operation of having one unit on outage and one on maintenance. The outage study revealed that neither the generators nor the transmission lines needed any reinforcement. The node and branch results shown in Appendix A1.1, for the base case. However, we note that the transformer located between nodes 80 and 81 is operating at its maximum limit. Next, we assess whether the 118-bus system requires any reactive support by applying the AC-OPF on it during four representative weeks. When we run the system without adding SVC units the system is capable of supplying the reactive demand, however when SVC are added the AC-OPF used them in order to minimize the objective function. The two runs are shown in Table 33 that clearly demonstrates a very slight increase in the LCOE due to the addition of the SVC on the system. There is also a corresponding very slight decrease in the CO_2 emissions. So the investment of $80.6

million in adding the SVC may be justified. These SVC were placed at several nodes as shown in Table 34. Figure 17 shows the total active power generated by the system versus time.

Table 33: 118-Bus Summary Table with SVC (50% Demand Increase)

Gen. size MW	SVC size MVAR	Total Investment M$	Total Capex M$/year	Total Opex M$/year	Fuel Cost M$/year	Total Energy Produced MWh	LCOE $/kWh	CO_2 ton/ year
8198	0.0	0.0	0.0	719.4	8209	38,185,746	0.2338	394,158
8198	1007	80.6	8.85	719	8194	38,113,816	0.2341	393,415

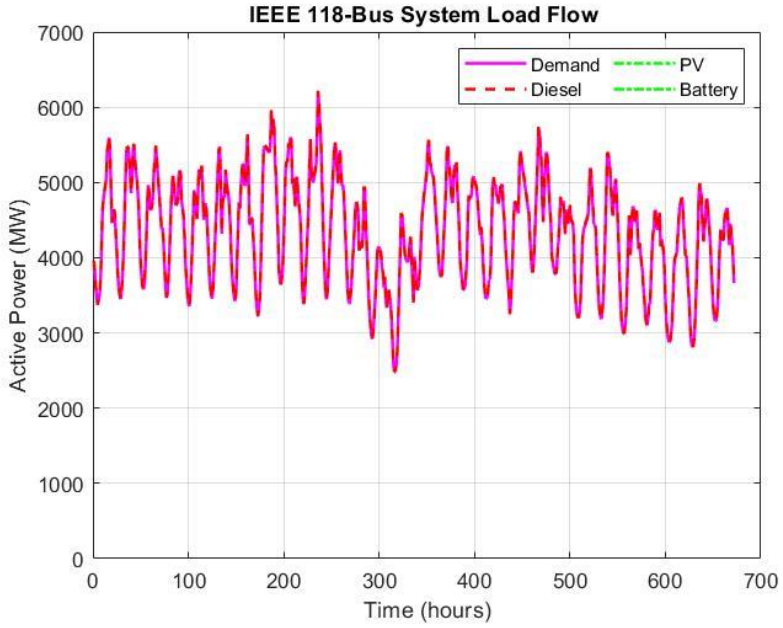

Figure 17: IEEE 118-Bus active demand versus time (50% Demand)

Table 34;: IEEE 118-Bus SVC Placements and Sizes (50% Demand)

Node	SVC Size	Node	SVC Size	Node	SVC Size
1	5.067	41	8.268	81	16.233
2	4.722	42	9.38	82	9.733
3	4.176	43	5.106	83	9.375
4	3.251	44	5.609	84	9.908
5	3.185	45	6.862	85	11.416
6	3.612	46	7.361	86	9.291
7	3.851	47	7.868	87	8.379
8	2.642	48	7.471	88	12.934
9	2.178	49	9.308	89	15.666
10	2.02	50	8.796	90	18.428
11	3.773	51	9.666	91	13.636
12	4.182	52	9.511	92	12.444
13	4.307	53	11.249	93	11.391
14	4.156	54	13.13	94	11.895
15	4.447	55	13.94	95	12.956
16	4.127	56	12.749	96	10.853
17	3.631	57	9.647	97	10.60
18	4.655	58	10.042	98	10.435
19	4.795	59	15.764	99	10.599
20	5.318	60	11.972	100	11.558
21	5.536	61	12.234	101	11.204
22	5.424	62	11.769	102	10.881
23	4.986	63	19.569	103	11.179
24	5.355	64	15.195	104	11.008
25	4.057	65	13.591	105	9.753
26	4.603	66	7.749	106	9.724
27	6.041	67	9.50	107	9.273
28	6.402	68	14.804	108	8.497
29	6.263	69	8.441	109	8.702
30	3.938	70	8.341	110	10.485
31	6.223	71	7.346	111	10.118
32	5.897	72	6.113	112	10.96
33	4.512	73	7.395	113	4.135
34	4.913	74	10.357	114	6.168
35	4.976	75	9.744	115	6.25
36	5.237	76	14.98	116	13.681
37	4.085	77	11.252	117	4.965
38	4.764	78	11.868	118	12.172
39	6.173	79	11.093		
40	7.594	80	10.218		

Table 35 below shows the timing of the different studies on the investigated systems. The outage study involved about 40 runs for the 30-Bus system and about 200 runs for the 118-bus system. The AC-OPF required 672 runs corresponding to the number of hours in the timeline. The runs were carried out on a laptop with Intel CPU core i7-11375H 3.30GHz with 16GB of RAM.

Table 35: Computer Timing of Different Studies

System / Time(sec)	Single DC-OPF	Outage	AC-OPF
5-Bus	0.0447	2.348	32.855
18-Bus	0.0741	-	37.486
30-Bus	0.0949	3.353	39.492
118-Bus	0.1217	9.399	129.386

CHAPTER IV

CONCLUSION & FUTURE WORK

In this thesis, we developed a methodology based on a transmission line outage study using a DC-OPF algorithm that makes the usage of fictitious generators in order to determine if generator or branch reinforcements are required. Then we used an AC-OPF formulation to determine the size and location of SVC that may be needed to help satisfy the reactive power demand of the system.

The transmission line outage methodology was applied to a 5-bus microgrid without renewable energy at peak demand, which showed that this system did require any reinforcement. When the peak demand was increased by 40%, the results showed that the transmission lines of the grid must be reinforced for it to become adequate. Then we illustrated how to apply this methodology to a system with renewable energy. The line outage study was applied at a particular critical hour of the 5-bus renewable grid that includes PV and batteries. The critical hour, when the system is most highly loaded, was determined using a transmission line performance (TLP) index calculated hourly for the selected timeline. The outage study at the critical hour resulted in multiple reinforcements based on the distribution of elements and sizing in the grid. After this, we applied the SVC analysis using the AC-OPF to test whether adding a reactive support to the system would reduce the usage of diesel fuel, and consequently reduce the LCOE and what effect this would have on the emission of CO_2.

To illustrate further our methodology, we carried out a similar analysis on the Younine 18 radial bus system which was presented with several alternatives to add renewable energy and battery storage. However, here the adequacy assessment of the system was done using a base-case analysis only. The reactive power assessment is

carried out in the same manner using the AC-OPF during the selected timeline. In addition we illustrated the implementation of the outage study on the IEEE 30-bus and 118-bus systems, as adjusted in terms of branch and generator data. For the 30-bus with 50% demand increase, it required generation and branch reinforcements. In addition, the system did require any SVC. The 118-bus system was also tested at its given demand peak and at 50% increase, which showed that this system did not require any reinforcement and any SVC. We then tested what would happen to the LCOE if we added SVC, which showed that such addition would increase slightly the LCOE but reduce slightly the CO2 emissions, driven by the lower use fossil fuel. When running the DC-OPF and AC-OPF we removed two units from the generators to reflect the usual practice of having one unit on maintenance and another on outage.

As a future work, we look forward to applying a cost to the carbon dioxide emission and implementing it in the LCOE calculation that will demonstrate that a system with SVC will reflect a lower LCOE. Also, we look forward to enhancing the SVC location and sizing methodology to find a more precise way to reallocate the SVC that was eliminated to the nearest node. In addition, we may modify the methodology to allow choosing the addition of SVC or the increase of inverters' sizes in a system with renewable energy. On the other hand, we are looking forward for improving the methodology to incorporate selected double line outage studies to reflect such a practice in some utilities. Additionally, we plan to integrate the generator outage methodology with the transmission line outage, which will contribute to a more secure and efficient grid. Furthermore, we plan to integrate renewable energy elements on the 30 and 118-bus to monitor their performance and understand how these elements may affect a complex grid.

APPENDIX

A1.0: IEEE 118-Data

Bus Data:

Node	Type	Active Demand (MW)	Reactive Demand (MVA)	Base KV
1	PQ	51	27	138
2	PV	20	9	138
3	PV	39	10	138
4	PQ	39	12	138
5	PV	0	0	138
6	PQ	52	22	138
7	PV	19	2	138
8	PQ	28	0	345
9	PV	0	0	345
10	PQ	0	0	345
11	PV	70	23	138
12	PQ	47	10	138
13	PV	34	16	138
14	PV	14	1	138
15	PQ	90	30	138
16	PV	25	10	138
17	PV	11	3	138
18	PQ	60	34	138
19	PQ	45	25	138
20	PV	18	3	138
21	PV	14	8	138
22	PV	10	5	138
23	PV	7	3	138
24	PQ	13	0	138
25	PQ	0	0	138
26	PQ	0	0	345
27	PQ	71	13	138
28	PV	17	7	138
29	PV	24	4	138
30	PV	0	0	345
31	PQ	43	27	138
32	PQ	59	23	138
33	PV	23	9	138
34	PQ	59	26	138
35	PV	33	9	138
36	PQ	31	17	138
37	PV	0	0	138
38	PV	0	0	345
39	PV	27	11	138
40	PQ	66	23	138
41	PV	37	10	138
42	PQ	96	23	138
43	PV	18	7	138
44	PV	16	8	138
45	PV	53	22	138
46	PQ	28	10	138
47	PV	34	0	138

48	PV	20	11	138
49	PQ	87	30	138
50	PV	17	4	138
51	PV	17	8	138
52	PV	18	5	138
53	PV	23	11	138
54	PQ	113	32	138
55	PQ	63	22	138
56	PQ	84	18	138
57	PV	12	3	138
58	PV	12	3	138
59	PQ	277	113	138
60	PV	78	3	138
61	PQ	0	0	138
62	PQ	77	14	138
63	PV	0	0	345
64	PV	0	0	345
65	PQ	0	0	345
66	PQ	39	18	138
67	PV	28	7	138
68	PV	0	0	345
69	RF	0	0	138
70	PQ	66	20	138
71	PV	0	0	138
72	PQ	12	0	138
73	PQ	6	0	138
74	PQ	68	27	138
75	PV	47	11	138
76	PQ	68	36	138
77	PQ	61	28	138
78	PV	71	26	138
79	PV	39	32	138
80	PQ	130	26	138
81	PV	0	0	345
82	PV	54	27	138
83	PV	20	10	138
84	PV	11	7	138
85	PQ	24	15	138
86	PV	21	10	138
87	PQ	0	0	161
88	PV	48	10	138
89	PQ	0	0	138
90	PQ	163	42	138
91	PQ	10	0	138
92	PQ	65	10	138
93	PV	12	7	138
94	PV	30	16	138
95	PV	42	31	138
96	PV	38	15	138
97	PV	15	9	138
98	PV	34	8	138
99	PQ	42	0	138
100	PQ	37	18	138
101	PV	22	15	138
102	PV	5	3	138

103	PQ	23	16	138
104	PQ	38	25	138
105	PQ	31	26	138
106	PV	43	16	138
107	PQ	50	12	138
108	PV	2	1	138
109	PV	8	3	138
110	PQ	39	30	138
111	PQ	0	0	138
112	PQ	68	13	138
113	PQ	6	0	138
114	PV	8	3	138
115	PV	22	7	138
116	PQ	184	0	138
117	PV	20	8	138
118	PV	33	15	138

Branch Data:

From	To	Resistance (PU)	Admittance (PU)	Susceptance (PU)	Rate (MVA)	Contingency
1	2	0.030	0.100	0.025	150	Y
1	3	0.013	0.042	0.011	150	Y
4	5	0.002	0.008	0.002	150	Y
3	5	0.024	0.108	0.028	150	Y
5	6	0.012	0.054	0.014	150	Y
6	7	0.005	0.021	0.006	150	Y
8	9	0.005	0.061	0.581	650	N
8	9	0.005	0.061	0.581	650	N
8	5	0.000	0.027	0.000	500	N
9	10	0.005	0.064	0.615	650	N
9	10	0.005	0.064	0.615	650	N
4	11	0.021	0.069	0.017	150	Y
5	11	0.020	0.068	0.017	150	Y
11	12	0.006	0.020	0.005	150	Y
2	12	0.019	0.062	0.016	150	Y
3	12	0.048	0.160	0.041	150	Y
7	12	0.009	0.034	0.009	150	Y
11	13	0.022	0.073	0.019	150	Y
12	14	0.022	0.071	0.018	150	Y
13	15	0.074	0.244	0.063	140	Y
14	15	0.060	0.195	0.050	150	Y
12	16	0.021	0.083	0.021	150	Y
15	17	0.026	0.087	0.022	150	Y
15	17	0.026	0.087	0.022	150	Y
16	17	0.045	0.180	0.047	150	Y
17	18	0.012	0.051	0.013	150	Y
18	19	0.011	0.049	0.011	150	Y
19	20	0.025	0.117	0.030	150	Y
15	19	0.012	0.039	0.010	150	Y
20	21	0.018	0.085	0.022	150	Y
21	22	0.021	0.097	0.025	150	Y
22	23	0.034	0.159	0.040	150	Y
23	24	0.027	0.098	0.025	150	Y
23	24	0.027	0.098	0.025	150	Y
23	25	0.031	0.160	0.043	150	Y
23	25	0.031	0.160	0.043	150	Y
26	25	0.000	0.038	0.000	400	N
25	27	0.064	0.326	0.088	130	Y

25	27	0.064	0.326	0.088	130	Y
27	28	0.019	0.086	0.022	150	Y
28	29	0.024	0.094	0.024	150	Y
30	17	0.000	0.039	0.000	400	N
8	30	0.004	0.050	0.514	800	Y
26	30	0.008	0.086	0.908	600	Y
17	31	0.047	0.156	0.040	150	Y
29	31	0.011	0.033	0.008	150	Y
23	32	0.063	0.231	0.059	150	Y
23	32	0.063	0.231	0.059	150	Y
31	32	0.030	0.099	0.025	150	Y
27	32	0.023	0.076	0.019	150	Y
15	33	0.038	0.124	0.032	150	Y
19	34	0.075	0.247	0.063	120	Y
35	36	0.002	0.010	0.003	150	Y
35	37	0.011	0.050	0.013	150	Y
33	37	0.042	0.142	0.037	150	Y
34	36	0.009	0.027	0.006	150	Y
34	37	0.005	0.019	0.005	150	Y
34	37	0.005	0.019	0.005	150	Y
38	37	0.000	0.038	0.000	400	N
37	39	0.032	0.106	0.027	150	Y
37	40	0.059	0.168	0.042	150	Y
30	38	0.005	0.054	0.422	650	Y
39	40	0.018	0.061	0.016	150	Y
40	41	0.015	0.049	0.012	150	Y
40	42	0.056	0.183	0.047	150	Y
41	42	0.041	0.135	0.034	150	Y
43	44	0.061	0.245	0.061	130	Y
34	43	0.041	0.168	0.042	150	Y
44	45	0.022	0.090	0.022	150	Y
45	46	0.040	0.136	0.033	150	Y
46	47	0.038	0.127	0.032	150	Y
46	48	0.060	0.189	0.047	150	Y
47	49	0.019	0.063	0.016	150	Y
42	49	0.072	0.323	0.086	130	Y
42	49	0.072	0.323	0.086	130	Y
45	49	0.068	0.186	0.044	150	Y
48	49	0.018	0.051	0.013	150	Y
49	50	0.027	0.075	0.019	150	Y
49	51	0.049	0.137	0.034	150	Y
51	52	0.020	0.059	0.014	150	Y
52	53	0.041	0.164	0.041	150	Y
53	54	0.026	0.122	0.031	150	Y
49	54	0.073	0.289	0.074	130	Y
49	54	0.087	0.291	0.073	130	Y
54	55	0.017	0.071	0.020	150	Y
54	56	0.006	0.019	0.004	130	Y
54	56	0.006	0.019	0.004	130	Y
55	56	0.005	0.015	0.004	150	Y
56	57	0.034	0.097	0.024	150	Y
50	57	0.047	0.134	0.033	150	Y
56	58	0.034	0.097	0.024	150	Y
51	58	0.026	0.072	0.018	150	Y
54	59	0.050	0.229	0.060	130	Y
56	59	0.083	0.251	0.066	140	Y
56	59	0.080	0.239	0.062	140	Y
55	59	0.047	0.216	0.056	150	Y
59	60	0.032	0.145	0.038	150	Y
59	61	0.033	0.150	0.039	150	Y
60	61	0.005	0.027	0.007	150	Y

60	61	0.005	0.027	0.007	150	Y
60	62	0.012	0.056	0.015	150	Y
61	62	0.008	0.038	0.010	150	Y
63	59	0.000	0.039	0.000	400	N
63	64	0.002	0.020	0.216	800	Y
64	61	0.000	0.027	0.000	500	N
38	65	0.009	0.099	1.046	490	Y
64	65	0.003	0.030	0.380	900	Y
49	66	0.018	0.092	0.025	150	Y
49	66	0.018	0.092	0.025	150	Y
62	66	0.048	0.218	0.058	130	Y
62	67	0.026	0.117	0.031	150	Y
65	66	0.000	0.037	0.000	400	N
66	67	0.022	0.102	0.027	150	Y
65	68	0.003	0.032	0.319	950	Y
65	68	0.003	0.032	0.319	950	Y
47	69	0.084	0.278	0.071	130	Y
49	69	0.099	0.324	0.083	130	Y
68	69	0.000	0.037	0.000	400	N
69	70	0.060	0.254	0.061	130	Y
69	70	0.060	0.254	0.061	130	Y
24	70	0.002	0.412	0.102	100	Y
70	71	0.009	0.036	0.009	150	Y
24	72	0.049	0.196	0.049	150	Y
71	72	0.045	0.180	0.044	150	Y
71	73	0.009	0.045	0.012	150	N
70	74	0.040	0.132	0.034	150	Y
70	75	0.043	0.141	0.036	150	Y
69	75	0.081	0.244	0.062	140	Y
69	75	0.081	0.244	0.062	140	Y
74	75	0.012	0.041	0.010	150	Y
76	77	0.044	0.148	0.037	150	Y
69	77	0.062	0.202	0.052	150	Y
69	77	0.062	0.202	0.052	150	Y
75	77	0.060	0.200	0.050	150	Y
77	78	0.008	0.025	0.006	150	Y
77	78	0.008	0.025	0.006	150	Y
78	79	0.005	0.024	0.006	150	Y
77	80	0.003	0.097	0.024	150	Y
77	80	0.003	0.097	0.024	150	Y
77	80	0.029	0.105	0.023	140	Y
79	80	0.016	0.070	0.019	150	Y
68	81	0.004	0.040	0.404	800	Y
68	81	0.004	0.040	0.404	800	Y
81	80	0.000	0.037	0.000	400	N
77	82	0.060	0.171	0.041	150	Y
77	82	0.060	0.171	0.041	150	Y
82	83	0.022	0.073	0.019	150	Y
82	83	0.022	0.073	0.019	150	Y
83	84	0.038	0.132	0.034	150	Y
83	85	0.043	0.148	0.035	150	Y
84	85	0.019	0.064	0.017	150	Y
85	86	0.035	0.123	0.032	150	N
86	87	0.028	0.207	0.045	150	N
85	88	0.020	0.102	0.028	150	Y
85	89	0.024	0.173	0.047	150	Y
88	89	0.014	0.071	0.019	150	Y
89	90	0.052	0.188	0.053	160	Y
89	90	0.026	0.150	0.066	200	Y
90	91	0.025	0.084	0.021	150	Y
89	92	0.020	0.126	0.052	200	Y

89	92	0.039	0.158	0.041	150	Y
91	92	0.039	0.127	0.033	150	Y
92	93	0.026	0.085	0.022	150	Y
92	94	0.048	0.158	0.041	150	Y
93	94	0.022	0.073	0.019	150	Y
94	95	0.013	0.043	0.011	150	Y
80	96	0.036	0.182	0.049	150	Y
82	96	0.032	0.106	0.027	150	Y
82	96	0.032	0.106	0.027	150	Y
94	96	0.027	0.087	0.023	150	Y
80	97	0.018	0.093	0.025	150	Y
80	98	0.024	0.108	0.029	150	Y
80	99	0.045	0.206	0.055	130	Y
92	100	0.065	0.295	0.075	140	Y
94	100	0.036	0.116	0.030	150	Y
94	100	0.036	0.116	0.030	150	Y
95	96	0.017	0.055	0.015	150	Y
96	97	0.017	0.089	0.024	150	Y
98	100	0.040	0.179	0.048	150	Y
99	100	0.018	0.081	0.022	150	Y
100	101	0.028	0.126	0.033	150	Y
92	102	0.012	0.056	0.015	150	Y
101	102	0.025	0.112	0.029	150	Y
100	103	0.032	0.105	0.027	150	Y
100	103	0.032	0.105	0.027	150	Y
100	104	0.045	0.204	0.054	150	Y
103	104	0.047	0.158	0.041	150	Y
103	105	0.054	0.163	0.041	150	Y
100	106	0.061	0.229	0.062	150	Y
104	105	0.010	0.038	0.010	150	Y
105	106	0.014	0.055	0.014	150	Y
105	107	0.053	0.183	0.047	150	Y
105	108	0.026	0.070	0.018	150	Y
106	107	0.053	0.183	0.047	150	Y
108	109	0.011	0.029	0.008	150	Y
103	110	0.039	0.181	0.046	150	Y
109	110	0.028	0.076	0.020	150	Y
110	111	0.022	0.076	0.020	150	N
110	112	0.049	0.128	0.031	120	N
110	112	0.049	0.128	0.031	120	N
17	113	0.009	0.030	0.008	150	Y
32	113	0.062	0.203	0.052	150	Y
32	114	0.014	0.061	0.016	150	Y
27	115	0.016	0.074	0.020	150	Y
114	115	0.002	0.010	0.003	150	Y
68	116	0.001	0.008	0.082	950	N
68	116	0.001	0.008	0.082	950	N
12	117	0.033	0.140	0.036	150	N
75	118	0.015	0.048	0.012	150	Y
76	118	0.016	0.054	0.014	150	Y

Generator Data:

Node	P_{min} (MW)	P_{max} (MW)	Q_{min} (MVAR)	Q_{max} (MVAR)
1	30	100	-16	33
4	30	100	-16	33
6	30	100	-16	33
8	30	100	-16	33
10	165	550	-90	181
12	55	185	-30	61

15	30	100	-16	33
18	30	100	-16	33
19	30	100	-16	33
24	30	100	-16	33
25	96	320	-53	105
26	124	414	-68	136
27	30	100	-16	33
31	32	107	-18	35
32	30	100	-16	33
34	30	100	-16	33
36	30	100	-16	33
40	30	100	-16	33
42	30	100	-16	33
46	35	119	-20	39
49	91	304	-50	100
54	44	148	-24	49
55	30	100	-16	33
56	30	100	-16	33
59	76	255	-42	84
61	78	260	-43	86
62	30	100	-16	33
65	147	491	-81	162
66	147	492	-81	162
69	240	800	-132	265
70	30	100	-16	33
72	30	100	-16	33
73	30	100	-16	33
74	30	100	-16	33
76	30	100	-16	33
77	30	100	-16	33
80	173	577	-95	190
85	30	100	-16	33
87	31	104	-17	34
89	210	700	-116	233
90	30	100	-16	33
91	30	100	-16	33
92	30	100	-16	33
99	30	100	-16	33
100	105	352	-58	116
103	42	140	-23	46
104	30	100	-16	33
105	30	100	-16	33
107	30	100	-16	33
110	30	100	-16	33
111	41	136	-22	45
112	30	100	-16	33
113	30	100	-16	33
116	30	100	-16	33

A1.1: IEEE 118-Bus at 50% Demand Increase

Bus Results:

Bus	Voltage		Generation		Load	
#	Magnitude	Angle(deg)	P(MW)	Q(MVAr)	P(MW)	Q(MVAr)
1	1	56.60	100	-	76.5	-
2	1	55.66	-	-	30	-
3	1	56.43	-	-	58.5	-
4	1	59.59	100	-	58.5	-
5	1	59.80	-	-	-	-
6	1	58.05	100	-	78	-
7	1	57.12	-	-	28.5	-
8	1	63.59	100	-	42	-
9	1	73.20	-	-	-	-
10	1	83.35	550	-	-	-
11	1	56.13	-	-	105	-
12	1	56.14	185	-	70.5	-
13	1	52.91	-	-	51	-
14	1	53.68	-	-	21	-
15	1	49.25	100	-	135	-
16	1	53.13	-	-	37.5	-
17	1	50.49	-	-	16.5	-
18	1	49.74	100	-	90	-
19	1	48.72	100	-	67.5	-
20	1	45.07	-	-	27	-
21	1	43.73	-	-	21	-
22	1	43.37	-	-	15	-
23	1	44.14	-	-	10.5	-
24	1	41.09	30	-	19.5	-
25	1	51.03	96	-	-	-
26	1	54.18	167.8	-	-	-
27	1	42.13	30	-	106.5	-
28	1	41.42	-	-	25.5	-
29	1	42.01	-	-	36	-
30	1	53.29	-	-	-	-
31	1	42.90	32	-	64.5	-
32	1	42.61	30	-	88.5	-
33	1	45.22	-	-	34.5	-
34	1	43.39	100	-	88.5	-
35	1	43.27	-	-	49.5	-
36	1	43.53	100	-	46.5	-
37	1	43.42	-	-	-	-
38	1	45.75	-	-	-	-
39	1	39.07	-	-	40.5	-
40	1	37.99	100	-	99	-
41	1	36.19	-	-	55.5	-
42	1	35.49	100	-	144	-
43	1	37.27	-	-	27	-
44	1	32.14	-	-	24	-
45	1	31.49	-	-	79.5	-
46	1	33.03	35	-	42	-
47	1	33.60	-	-	51	-
48	1	35.09	-	-	30	-
49	1	36.51	304	-	130.5	-
50	1	34.53	-	-	25.5	-
51	1	31.98	-	-	25.5	-
52	1	30.96	-	-	27	-
53	1	30.65	-	-	34.5	
54	1	32.82	148	-	169.5	
55	1	32.92	100	-	94.5	
56	1	32.80	100	-	126	
57	1	32.94	-	-	18	

58	1	31.90	-	-	18	
59	1	34.25	255	-	415.5	
60	1	37.73	-	-	117	
61	1	38.76	260	-	-	
62	1	38.55	100	-	115.5	
63	1	36.54	-	-	-	
64	1	37.78	-	-	-	
65	1	38.54	491	-	-	
66	1	41.74	492	-	58.5	
67	1	38.95	-	-	42	
68	1	31.79	-	-	-	
69	1	30.00	241	-	-	
70	1	26.13	30	-	99	
71	1	27.93	-	-	-	
72	1	34.87	30	-	18	
73	1	28.47	30	-	9	
74	1	20.80	30	-	102	
75	1	20.83	-	-	70.5	
76	1	16.43	30	-	102	
77	1	18.15	30	-	91.5	
78	1	17.34	-	-	106.5	
79	1	17.22	-	-	58.5	
80	1	19.23	173	-	195	
81	1	27.16	-	-	-	
82	1	13.85	-	-	81	
83	1	14.28	-	-	30	
84	1	15.67	-	-	16.5	
85	1	16.95	30	-	36	
86	1	16.92	-	-	31.5	
87	1	20.60	31	-	-	
88	1	18.23	-	-	72	-
89	1	22.05	474.2	-	-	-
90	1	15.27	100	-	244.5	-
91	1	15.40	30	-	15	-
92	1	14.51	30	-	97.5	-
93	1	12.60	-	-	18	-
94	1	11.71	-	-	45	-
95	1	11.42	-	-	63	-
96	1	13.03	-	-	57	-
97	1	15.46	-	-	22.5	-
98	1	14.16	-	-	51	-
99	1	12.22	30	-	63	-
100	1	10.99	105	-	55.5	-
101	1	11.04	-	-	33	-
102	1	13.19	-	-	7.5	-
103	1	8.73	42	-	34.5	-
104	1	7.17	30	-	57	-
105	1	6.67	100	-	46.5	-
106	1	5.45	-	-	64.5	-
107	1	3.70	30	-	75	-
108	1	5.42	-	-	3	-
109	1	4.95	-	-	12	-
110	1	4.24	30	-	58.5	-
111	1	6.01	41	-	-	-
112	1	1.60	30	-	102	-
113	1	50.84	100	-	9	-
114	1	41.57	-	-	12	-
115	1	41.47	-	-	33	-
116	1	31.22	30	-	276	-
117	1	53.73	-	-	30	-
118	1	18.04	-	-	49.5	-

Branch Results:

From	To	Active From (MW)	Reactive From (MVAR)	Active To (MW)	Reactive To (MVAR)
1	2	16.42	0.00	-16.42	0.00
1	3	7.08	0.00	-7.08	0.00
4	5	-46.22	0.00	46.22	0.00
3	5	-54.56	0.00	54.56	0.00
5	6	56.60	0.00	-56.60	0.00
6	7	78.60	0.00	-78.60	0.00
8	9	-275.00	0.00	275.00	0.00
8	9	-275.00	0.00	275.00	0.00
8	5	251.28	0.00	-251.28	0.00
9	10	-275.00	0.00	275.00	0.00
9	10	-275.00	0.00	275.00	0.00
4	11	87.72	0.00	-87.72	0.00
5	11	93.90	0.00	-93.90	0.00
11	12	-0.47	0.00	0.47	0.00
2	12	-13.58	0.00	13.58	0.00
3	12	3.14	0.00	-3.14	0.00
7	12	50.10	0.00	-50.10	0.00
11	13	77.09	0.00	-77.09	0.00
12	14	60.65	0.00	-60.65	0.00
13	15	26.09	0.00	-26.09	0.00
14	15	39.65	0.00	-39.65	0.00
12	16	63.04	0.00	-63.04	0.00
15	17	-24.76	0.00	24.76	0.00
15	17	-24.76	0.00	24.76	0.00
16	17	25.54	0.00	-25.54	0.00
17	18	26.07	0.00	-26.07	0.00
18	19	36.07	0.00	-36.07	0.00
19	20	54.51	0.00	-54.51	0.00
15	19	23.62	0.00	-23.62	0.00
20	21	27.51	0.00	-27.51	0.00
21	22	6.51	0.00	-6.51	0.00
22	23	-8.49	0.00	8.49	0.00
23	24	54.14	0.00	-54.14	0.00
23	24	54.14	0.00	-54.14	0.00
23	25	-75.20	0.00	75.20	0.00
23	25	-75.20	0.00	75.20	0.00
26	25	149.75	0.00	-149.75	0.00
25	27	47.67	0.00	-47.67	0.00
25	27	47.67	0.00	-47.67	0.00
27	28	14.49	0.00	-14.49	0.00
28	29	-11.01	0.00	11.01	0.00
30	17	131.05	0.00	-131.05	0.00
8	30	356.72	0.00	-356.72	0.00
26	30	18.05	0.00	-18.05	0.00
17	31	84.73	0.00	-84.73	0.00
29	31	-47.01	0.00	47.01	0.00
23	32	11.57	0.00	-11.57	0.00
23	32	11.57	0.00	-11.57	0.00
31	32	5.23	0.00	-5.23	0.00
27	32	-11.13	0.00	11.13	0.00
15	33	56.63	0.00	-56.63	0.00
19	34	37.68	0.00	-37.68	0.00
35	36	-44.35	0.00	44.35	0.00
35	37	-5.15	0.00	5.15	0.00
33	37	22.13	0.00	-22.13	0.00

34	36	-9.15	0.00	9.15	0.00
34	37	-2.59	0.00	2.59	0.00
34	37	-2.59	0.00	2.59	0.00
38	37	116.13	0.00	-116.13	0.00
37	39	71.57	0.00	-71.57	0.00
37	40	56.35	0.00	-56.35	0.00
30	38	243.72	0.00	-243.72	0.00
39	40	31.07	0.00	-31.07	0.00
40	41	64.56	0.00	-64.56	0.00
40	42	23.86	0.00	-23.86	0.00
41	42	9.06	0.00	-9.06	0.00
43	44	36.51	0.00	-36.51	0.00
34	43	63.51	0.00	-63.51	0.00
44	45	12.51	0.00	-12.51	0.00
45	46	-19.84	0.00	19.84	0.00
46	47	-7.79	0.00	7.79	0.00
46	48	-19.05	0.00	19.05	0.00
47	49	-81.40	0.00	81.40	0.00
42	49	-5.54	0.00	5.54	0.00
42	49	-5.54	0.00	5.54	0.00
45	49	-47.14	0.00	47.14	0.00
48	49	-49.05	0.00	49.05	0.00
49	50	46.13	0.00	-46.13	0.00
49	51	57.73	0.00	-57.73	0.00
51	52	30.35	0.00	-30.35	0.00
52	53	3.35	0.00	-3.35	0.00
53	54	-31.15	0.00	31.15	0.00
49	54	22.29	0.00	-22.29	0.00
49	54	22.13	0.00	-22.13	0.00
54	55	-2.31	0.00	2.31	0.00
54	56	2.45	0.00	-2.45	0.00
54	56	2.45	0.00	-2.45	0.00
55	56	13.93	0.00	-13.93	0.00
56	57	-2.63	0.00	2.63	0.00
50	57	20.63	0.00	-20.63	0.00
56	58	16.12	0.00	-16.12	0.00
51	58	1.88	0.00	-1.88	0.00
54	59	-10.82	0.00	10.82	0.00
56	59	-10.07	0.00	10.07	0.00
56	59	-10.58	0.00	10.58	0.00
55	59	-10.74	0.00	10.74	0.00
59	60	-41.93	0.00	41.93	0.00
59	61	-52.53	0.00	52.53	0.00
60	61	-66.65	0.00	66.65	0.00
60	61	-66.65	0.00	66.65	0.00
60	62	-25.62	0.00	25.62	0.00
61	62	9.63	0.00	-9.63	0.00
63	59	108.25	0.00	-108.25	0.00
63	64	-108.25	0.00	108.25	0.00
64	61	-64.53	0.00	64.53	0.00
38	65	127.59	0.00	-127.59	0.00
64	65	-43.73	0.00	43.73	0.00
49	66	-99.27	0.00	99.27	0.00
49	66	-99.27	0.00	99.27	0.00
62	66	-25.53	0.00	25.53	0.00
62	67	-5.96	0.00	5.96	0.00
65	66	-161.47	0.00	161.47	0.00
66	67	47.96	0.00	-47.96	0.00
65	68	368.16	0.00	-368.16	0.00
65	68	368.16	0.00	-368.16	0.00
47	69	22.61	0.00	-22.61	0.00

49	69	35.09	0.00	-35.09	0.00
68	69	90.33	0.00	-90.33	0.00
69	70	26.59	0.00	-26.59	0.00
69	70	26.59	0.00	-26.59	0.00
24	70	63.43	0.00	-63.43	0.00
70	71	-88.34	0.00	88.34	0.00
24	72	55.34	0.00	-55.34	0.00
71	72	-67.34	0.00	67.34	0.00
71	73	-21.00	0.00	21.00	0.00
70	74	70.38	0.00	-70.38	0.00
70	75	65.57	0.00	-65.57	0.00
69	75	65.57	0.00	-65.57	0.00
69	75	65.57	0.00	-65.57	0.00
74	75	-1.62	0.00	1.62	0.00
76	77	-20.30	0.00	20.30	0.00
69	77	102.35	0.00	-102.35	0.00
69	77	102.35	0.00	-102.35	0.00
75	77	23.39	0.00	-23.39	0.00
77	78	57.52	0.00	-57.52	0.00
77	78	57.52	0.00	-57.52	0.00
78	79	8.54	0.00	-8.54	0.00
77	80	-19.41	0.00	19.41	0.00
77	80	-19.41	0.00	19.41	0.00
77	80	-17.93	0.00	17.93	0.00
79	80	-49.96	0.00	49.96	0.00
68	81	200.00	0.00	-200.00	0.00
68	81	200.00	0.00	-200.00	0.00
81	80	400.00	0.00	-400.00	0.00
77	82	44.00	0.00	-44.00	0.00
77	82	44.00	0.00	-44.00	0.00
82	83	-10.08	0.00	10.08	0.00
82	83	-10.08	0.00	10.08	0.00
83	84	-18.56	0.00	18.56	0.00
83	85	-31.59	0.00	31.59	0.00
84	85	-35.06	0.00	35.06	0.00
85	86	0.50	0.00	-0.50	0.00
86	87	-31.00	0.00	31.00	0.00
85	88	-21.75	0.00	21.75	0.00
85	89	-51.40	0.00	51.40	0.00
88	89	-93.75	0.00	93.75	0.00
89	90	62.96	0.00	-62.96	0.00
89	90	78.76	0.00	-78.76	0.00
90	91	-2.78	0.00	2.78	0.00
89	92	104.10	0.00	-104.10	0.00
89	92	83.23	0.00	-83.23	0.00
91	92	12.22	0.00	-12.22	0.00
92	93	39.23	0.00	-39.23	0.00
92	94	30.89	0.00	-30.89	0.00
93	94	21.23	0.00	-21.23	0.00
94	95	11.75	0.00	-11.75	0.00
80	96	59.50	0.00	-59.50	0.00
82	96	13.58	0.00	-13.58	0.00
82	96	13.58	0.00	-13.58	0.00
94	96	-26.39	0.00	26.39	0.00
80	97	70.48	0.00	-70.48	0.00
80	98	81.92	0.00	-81.92	0.00
80	99	59.40	0.00	-59.40	0.00
92	100	20.82	0.00	-20.82	0.00
94	100	10.87	0.00	-10.87	0.00
94	100	10.87	0.00	-10.87	0.00
95	96	-51.25	0.00	51.25	0.00

96	97	-47.98	0.00	47.98	0.00
98	100	30.92	0.00	-30.92	0.00
99	100	26.40	0.00	-26.40	0.00
100	101	-0.62	0.00	0.62	0.00
92	102	41.12	0.00	-41.12	0.00
101	102	-33.62	0.00	33.62	0.00
100	103	37.54	0.00	-37.54	0.00
100	103	37.54	0.00	-37.54	0.00
100	104	32.70	0.00	-32.70	0.00
103	104	17.22	0.00	-17.22	0.00
103	105	22.12	0.00	-22.12	0.00
100	106	42.22	0.00	-42.22	0.00
104	105	22.92	0.00	-22.92	0.00
105	106	38.96	0.00	-38.96	0.00
105	107	28.32	0.00	-28.32	0.00
105	108	31.25	0.00	-31.25	0.00
106	107	16.68	0.00	-16.68	0.00
108	109	28.25	0.00	-28.25	0.00
103	110	43.25	0.00	-43.25	0.00
109	110	16.25	0.00	-16.25	0.00
110	111	-41.00	0.00	41.00	0.00
110	112	36.00	0.00	-36.00	0.00
110	112	36.00	0.00	-36.00	0.00
17	113	-20.22	0.00	20.22	0.00
32	113	-70.78	0.00	70.78	0.00
32	114	29.51	0.00	-29.51	0.00
27	115	15.49	0.00	-15.49	0.00
114	115	17.51	0.00	-17.51	0.00
68	116	123.00	0.00	-123.00	0.00
68	116	123.00	0.00	-123.00	0.00
12	117	30.00	0.00	-30.00	0.00
75	118	101.20	0.00	-101.20	0.00
76	118	-51.70	0.00	51.70	0.00

REFERENCES

[1] F. Perez, L. de Medeiros and A. Pedretti, "Active and Reactive Power control in a grid-connected Microgrid with Energy Storage Management," *2019 IEEE PES Innovative Smart Grid Technologies Conference - Latin America (ISGT Latin America)*, Gramado, Brazil, 2019, pp. 1-6, doi: 10.1109/ISGT-LA.2019.8895366.

[2] V. Komoni, I. Krasniqi, G. K. dhe and A. Alidemaj, "Control active and reactive power flow with UPFC connected in transmission line," *8th Mediterranean Conference on Power Generation, Transmission, Distribution and Energy Conversion (MEDPOWER 2012)*, Cagliari, 2012, pp. 1-6, doi: 10.1049/cp.2012.2015

[3] C Venkata & Manjunatha, A. (2021). "Compensation of Reactive Power in Grid-Connected Solar PV Array System Using STATCOM and Fixed Capacitor Bank", Int. Journal of Engineering Trends and Technology, Vol 69, Issue 10, 128-136, Oct. 2021, doi: 10.14445/22315381/IJETT-V69I10P216.

[4] Y. Guo, S. Sheng, N. Anglani and B. Lehman, "Optimal Power Management for Grid-Connected Microgrid Considering Modelling of Different Electricity Cost and Battery Degradation Cost," *2019 20th Workshop on Control and Modeling for Power Electronics (COMPEL)*, Toronto, ON, Canada, 2019, pp. 1-7, doi: 10.1109/COMPEL.2019.8769640.

[5] B. M. Eid, N. A. Rahim and J. Selvaraj, "Distributed photovoltaic generator performing reactive power compensation," *2013 IEEE Conference on Clean Energy and Technology (CEAT)*, Langkawi, Malaysia, 2013, pp. 38-41, doi: 10.1109/CEAT.2013.6775596.

[6] Parvathy S., K.C. Sindhu Thampatty, "Dynamic Modeling and Control of UPFC for Power Flow Control," Procedia Technology, Volume 21, 2015, Pages 581-588, ISSN 2212-0173

[7] R. E. Ramli, M. Awad and R. A. Jabr, "Ordinal optimization for optimal Capacitor Placement and network reconfiguration in radial distribution networks," *2012 IEEE International Conference on Systems, Man, and Cybernetics (SMC)*, Seoul, Korea (South), 2012, pp. 1712-1717, doi: 10.1109/ICSMC.2012.6377984.

[8] Karaki, Sami & Dinnawi, Rafika & Jabr, Rabih & Chedid, R. & Panik, Ferdinand. (2015). Fuel Cell Hybrid Electric Vehicle Sizing using Ordinal Optimization. SAE International Journal of Passenger Cars - Electronic and Electrical Systems. 8. 10.4271/2015-01-0155.

[9] A. Dhaneria, "Grid Connected PV System with Reactive Power Compensation for the Grid," *2020 IEEE Power & Energy Society Innovative Smart Grid Technologies Conference (ISGT)*, Washington, DC, USA, 2020, pp. 1-5, doi: 10.1109/ISGT45199.2020.9087728.

[10] H. Barot and K. Bhattacharya, "Optimal Reactive Power Planning and Compensation Effects on Transmission Loss Components," *2007 IEEE Power*

Engineering Society General Meeting, Tampa, FL, USA, 2007, pp. 1-7, doi: 10.1109/PES.2007.386161.

[11] Kahourzade, Solmaz & Mahmoudi, Amin & Mokhlis, Hazlie. (2014). A comparative study of multi-objective optimal power flow based on particle swarm, evolutionary programming, and genetic algorithm. Electrical Engineering. 97. 10.1007/s00202-014-0307-0.

[12] A. A. Alabduljabbar and J. V. Milanovic, "Generation Costs Reduction Through Optimal Allocation of FACTS Devices Using Low Discrepancy Sequences," *2006 IEEE PES Power Systems Conference and Exposition*, Atlanta, GA, USA, 2006, pp. 946-951, doi: 10.1109/PSCE.2006.296440.

[13] R. Jena, S. Chirantan, S. C. Swain and P. C. Panda, "Load flow analysis and optimal allocation of SVC in nine bus power system," *2018 Technologies for Smart-City Energy Security and Power (ICSESP)*, Bhubaneswar, India, 2018, pp. 1-5, doi: 10.1109/ICSESP.2018.8376741.

[14] P. S. V. Prabhakar, R. Krishan and D. R. Pullaguram, "Static Security Assessment of Large Power Systems Under N-1-1 Contingency," *2022 22nd National Power Systems Conference (NPSC)*, New Delhi, India, 2022, pp. 35-40, doi: 10.1109/NPSC57038.2022.10069705.

[15] Kumar, Uday and H. R. Sudarshana Reddy. “Contingency Ranking in Modern Power System by Exact and Precise Method”, *International journal of Innovative Research in Electrical, Electronics, Instrumentation and Control Engineering*, vol. 3, Issue 5, May, 2015, doi: 10.17148/IJIREEICE.2015.3555.

[16] P. Maghouli, S. H. Hosseini, M. O. Buygi and M. Shahidehpour, "A Multi-Objective Framework for Transmission Expansion Planning in Deregulated Environments," in IEEE Transactions on Power Systems, vol. 24, no. 2, pp. 1051-1061, May 2009, doi: 10.1109/TPWRS.2009.2016499.

[17] Mahmoudabadi, Amin. (2012). A New Model for Transmission Network Expansion and Reactive Power Planning in a Deregulated Environment. Engineering. 04. 119-125. 10.4236/eng.2012.42015.

[18] Alvarez R., Rahmann C., Palma-Behnke R., Estévez P.A., “A novel meta-heuristic model for the multi-year transmission network expansion planning” , (2019) International Journal of Electrical Power and Energy Systems, 107, pp. 523 - 537, Cited 22 times, DOI: 10.1016/j.ijepes.2018.12.022

[19] Y. Gu and J. McCalley, "Market-based transmission expansion planning," *2011 IEEE/PES Power Systems Conference and Exposition*, Phoenix, AZ, USA, 2011, pp. 1-9, doi: 10.1109/PSCE.2011.5772507.

[20] M. Mahdavi, C. Sabillon Antunez, M. Ajalli and R. Romero, "Transmission Expansion Planning: Literature Review and Classification," in *IEEE Systems Journal*, vol. 13, no. 3, pp. 3129-3140, Sept. 2019, doi: 10.1109/JSYST.2018.2871793.

[21] O’Neill, Richard & Krall, Eric & Hedman, Kory & Oren, Shmuel. (2013). A model and approach to the challenge posed by optimal power systems planning.

Mathematical Programming. Series A. Series B. 140. 10.1007/s10107-013-0695-3.

[22] G. Latorre, R. D. Cruz, J. M. Areiza and A. Villegas, "Classification of publications and models on transmission expansion planning," in *IEEE Transactions on Power Systems*, vol. 18, no. 2, pp. 938-946, May 2003, doi: 10.1109/TPWRS.2003.811168.

[23] P. Kundur, *Power System Stability and Control*. New York, NY, USA: McGraw-Hill, 1994.

[24] Wafaa Salloum, “Sustainable Energy Resource Planning in a Miro-Grid”, Master’s Thesis, American University of Beirut, Beirut, Lebanon, June 2024.

[25] Ramassamy V., Feldman D., Desai J, and Margolis R. (2021): US Solar Photovoltaic System and Energy Storage Cost Benchmarks: Q1 2021, NREL/ TP-7A40-80694, November 2021.

[26] EIA (2020). Cost and Performance Characteristics of New Generating Technologies, Annual Energy Outlook 2020, Energy Information Administration.

[27] American Electric Power System in the Midwestern US of December 1962 IEEE 30 Bus data, https://labs.ece.uw.edu/pstca/pf30/pg_tca30bus.htm

[28] American Electric Power System in the Midwestern US of December 1962 IEEE 118 Bus data, https://labs.ece.uw.edu/pstca/pf118/pg_tca118bus.htm

[29] Glover J.D., Sarma M. S., Overbye J. T. (2012). *Power System Analysis and Design*, Fifth Ed., Stamford, CT, USA: Cengage Learning, 2012.